Selective DCP detection with xanthene derivatives by carbonyl phosphorylation

Kanhu Charan Behera[a, b] and Bamaprasad Bag[a,*]

[a]Materials Chemistry Department, CSIR-Institute of Minerals and Materials Technology, P.O.: R.R.L., Bhubaneswar-751013, Odisha, India. Fax: (+) 91 674 258 1637; Tel: (+ 91) 674 237 9254, Email: *bpbag@immt.res.in*
[b]co-affiliation: Department of Chemistry, Utkal University, P.O.: Bhubaneswar-751013, Odisha, India

Electronic Supplementary Information

Experimental Section.

Materials and methods

All the reagent grade chemicals were used besides purification unless otherwise detailed. Rhodamine 6G, Fluorescein, 4-diethylaminobenzaldehyde, 4-(diethylamino-)salicylaldehyde, hydrazine monohydrate, *p*-toluene sulfonyl chloride(Tosyl chloride), Benzoyl chloride and Diethyl-chlorophosphate (DCP) were obtained from sigma Aldrich (India) Pvt. Ltd and used as received. Anhydrous sodium sulphate, silica gel for column chromatography, acids and the organic solvents were received from Spectrochem Pvt. Ltd (India). Various pesticides such as Acephate, Monochrotophos, Thimet, Carbofuran, Quinalphos, Chlorpyriphos, Cartaphy, Cypermethrin, Dichlorvos were purchased from local chemical store. All the solvents were freshly distilled prior to use for absorption and fluorescence measurements. The compounds were characterized by elemental analyses, ^{1}H NMR, ^{13}C NMR and mass (ESI) spectroscopy. ^{1}H NMR and ^{13}C NMR spectra were recorded on a JEOL JNM-AL400 FT V4.0 AL 400 at 400 MHz and 100 MHz respectively instrument in DMSO-d_6 with Me_4Si as internal standard. Electrospray mass spectral data were recorded on a maXis impact ESI–QTOF Instant Expertise mass spectrometer. Melting points were determined with a melting point apparatus of Stuart SM120, India and were uncorrected. FT-IR spectra were recorded on a Perkin Elmer Spectrum GX spectrometer. UV-visible absorption spectra were recorded on a Perkin Elmer Lambda 650 UV/VIS spectrophotometer at 298K. Steady-state fluorescence spectra were obtained with a Fluoromax 4P spectrofluorometer at 298 K. Fluorescence quantum yields were determined[RS1] in each case by comparing the corrected spectrum with that of Rhodamine 6G (ϕ_F=0.95)[RS2] in EtOH by taking the area under total emission. Limit of Detection(LOD) and limit of Quantification of probe-DCP interaction were determined following previously reported[RS3] procedures. The association constant (Ka) of the complexes were determined from change in absorbance or fluorescence resulted from titration of dilute solutions (~10^{-5}- 10^{-6} M) of probes against DCP solution following an equation reported[RS4] for a 1:1(probe: DCP) stoichiometry of complex formation.

The time resolved fluorescence measurements were evaluated in an Edinburgh FLS980 photoluminescence spectrometer through time correlated single photon counting (TCSPC) technique.The exponential decay curve of **1**, **2** and **3** and their corresponding adducts were fitted appropriately with a bi-exponential equation $Y = A+B_1 \exp(-t/\tau_1) + B_2 \exp(-t/\tau_2)$ to obtain best goodness-of-fit χ^2 value. The average life time (τ_{av}) was calculated following the equations depicted in literature[RS5].

X-ray diffraction data for single crystals of **1**, **2** and **3** were collected with a Bruker Apex II CCD diffractometer using graphite-monochromated MoK_α radiation (λ = 0.71073 Å) at 273 K (for **1** and **2**) and 102K (for **3**) with diffraction measurement methods of ϕ and ω scans. The cell parameters in each case were determined by least-squares refinement of the diffractometer with Bruker SAINT programme. The linear absorption coefficients, scattering factors for the atoms, and the anomalous dispersion corrections were taken from International Tables for X-ray Crystallography. The data reduction computation were also done using Bruker SAINT program. The structures were solved by the direct method using SHELXS 97 and were refined on F^2 by full-matrix least-squares technique using the SHELXL-2013 program package. In each case, some of the H atoms could be located in the difference maps while the rest were calculated assuming ideal geometries of the atoms concerned. All non-hydrogen atoms were refined anisotropically while the hydrogen atoms were treated as riding atoms using SHELXTL default parameters.

Quantum chemical calculations (gas phase / vacuum) for ground state energy minimized structures for the probes(**1**, **2** and **3**), all pesticides (Scheme S1) and adducts (**1**-DP, **2**-DP) were done employing density functional theory(DFT) in a Gaussian 09W program package. The ground state structural elucidation involved in optimization using DFT based Beck-3 Lee Young Parr (B3LYP) functional where 6-311G basis sets were used.

The commonly adapted TLC paper methodology was followed to validate the probe's capabilities in DCP detection**.** TLC plates (3 cm x 1 cm) were prepared by dipping TLC paper into solution of probe **1** and **2** (10 µM) in EtOH- H_2O (1:1 v/v, PBS, pH = 7.1) for 10 minutes and subsequently air dried. The dry paper strips are found to be colourless and non-fluorescent. Subsequently, 3mL of DCP solution of various concentration (0µM, 10µM, 100µM, 1mM from left to right) taken in four different centrifuge tubes and placed the TLC plates pre-loaded with probe **1** and **2** inside the individual tubes and capped. The observations, in form of colourization, were recorded within 5-10 minutes after exposure.

In order to explore efficacy of these probes in detection of DCP in real samples, the soil samples were taken, mixed with a solution of DCP (100µM) and dried. The soil samples were then stirred in EtOH-H_2O mixture for 1h and filtered. The filtrate was added with known concentration of **1** and their spectra were recorded. A colourization of the solution rendered visual display of qualitative DCP detection.

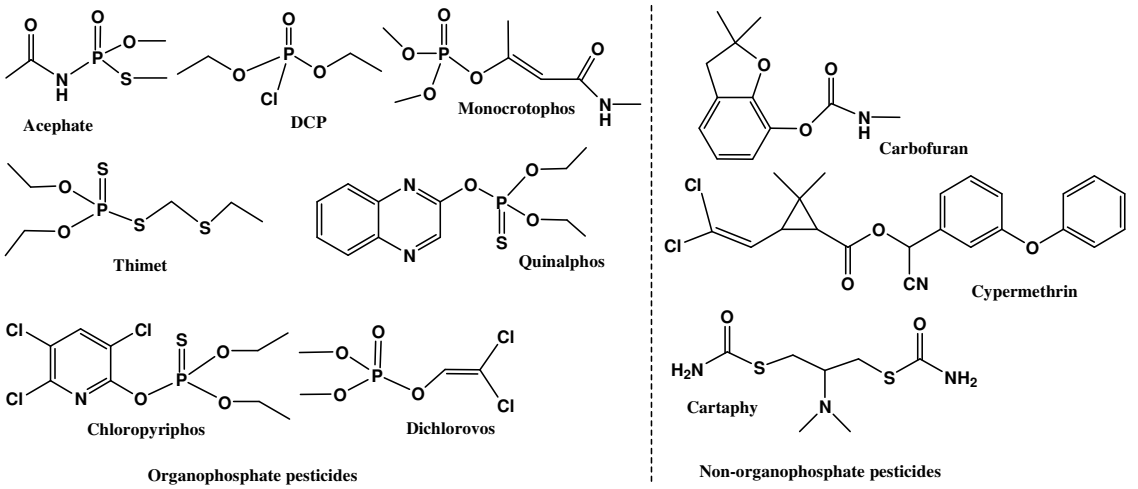

Scheme S1: Chemical structures of pesticides used in this study.

Synthesis

The compounds were synthesized as shown in the scheme (Scheme S2).

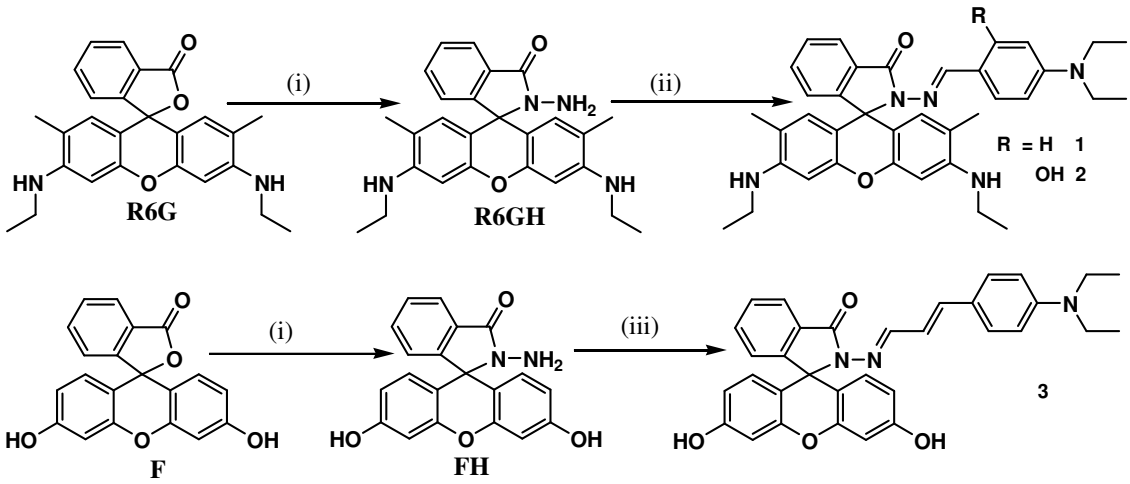

Reaction Conditions: (i) Hydrazine hydrate, EtOH, reflux, 6-8h; (ii) MeOH, 4-diethylamino-benzaldehyde (for **1**) or 4-(diethylamino)-salicylaldehyde(for **2**), reflux 6h; (iii) EtOH, trans-(diethyl amine)-cinnamaldehyde, glacial acetic acid, reflux 6h

Scheme S2: Synthetic route to the compounds (**1**-**3**)

Synthesis of rhodamine hydrazide (**R6GH**)

Although synthesis of R6GH is known[RS6], it was synthesized from rhodamine-6G following the procedure described here. To a stirring solution of Rhodamine 6G (1.916g, 4 mmol) dissolved in ethanol(30 mL), an ethanolic solution(30 mL) of hydrazine monohydrate (1.318 mL, 26 mmol) was added drop-wise and heated to reflux for 6h where decolorization of reddish coloured solution was observed. The reaction mixture was then brought back to RT

and the solvent was removed under vacuum. Water (20 mL) was added to the residual mass followed by extraction with $CHCl_3$ (20 mL × 2). The solvent of the combined organic phases, after drying over Na_2SO_4, was removed under reduced pressure to get the desired **R6GH** as light brown coloured solid; which was used directly for subsequent syntheses of **1** and **2**.

General procedure for Synthesis of **1** and **2**

To a stirring solution of **R6GH**(0.428g, 1.0mmol) in MeOH (30 mL), a methanolic solution(20mL) of the aldehyde [4-diethylamino benzaldehyde (0.177g, 1.0mmol) for **1** and 4-(diethylamino)salicylaldehyde(0.193g, 1.0mmol) for **2**] was added, and heated to reflux for 6h with constant stirring until a pale yellow coloured precipitate crashed out of the solution. It was allowed to cool to room temperature and allowed to precipitate further by keeping at ice temperature over night. The crude solid was isolated by filtration, washed with water and further extracted with $CHCl_3$ (3 ×30 mL). The organic layers, after drying over Na_2SO_4, were evaporated under reduced pressure to obtain the pale yellow coloured solid as desired products (**1** and **2** respectively), which were further purified by passing through a column of neutral alumina (100-200 mesh) with chloroform and methanol mixture(variable proportions) as eluent. Their solution in ethanol afforded their single crystals (**1** and **2**) suitable for X-ray diffraction through slow evaporation technique.

1. Yield =0.47g (79%), m. p. = > 200^oC; ESI-MS($C_{37}H_{41}N_5O_2$) m/z$^+$(%): 588.48 $[M+1]^+$ (100); 589.48 $[M+2]^+$ (48); ^{1}H NMR (400MHz, DMSO-d_6, 25°C, TMS, δ):8.54(s, 1H), 7.82(d, 1H, J = 2.0Hz) 7.49(m, 2H), 7.16(d, 2H, J = 9.2Hz), 6.97(dd, 1H, J_1 = 4.4Hz, J_2 = 2.0 Hz), 6.56(d, 2H, J = 8.8Hz), 6.30(s, 2H), 6.14(s, 2H), 4.98(t, 2H, J =6.0 Hz), 3.28(dd, 4H, J_1= 8.8Hz, J_2= 5.2 Hz), 3.08(p, 4H, J_1 = 6.8Hz, J_2 = 1.2Hz), 1.83(s, 6H), 1.17(t, 6H, J = 7.2Hz), 1.02(t, 6H, J = 6.8Hz); ^{13}C NMR (100MHz, DMSO-d_6, 25°C, TMS, δ):163.1, 151.4, 150.9, 148.9, 147.6, 133.1, 129.2, 128.4, 126.8, 123.5, 122.6, 120.8, 117.9, 110.9, 105.3, 95.7, 65.7, 43.6, 37.4, 16.9, 14.1, 12.3 ; Anal. calcd. for $C_{37}H_{41}N_5O_2$ (M_w = 587.33), (%): C, 75.61; H, 7.03; N, 11.92; found (%): C, 75.36; H, 7.13; N, 11.59; IR: $\upsilon_{str.}$(C=O): 1708 cm^{-1} (KBr). CCDC No. to crystal structure of **1**: 1963360.

2. Yield = 0.46g (76 %), m. p. = >200 ^{o}C , ESI-MS ($C_{37}H_{41}N_5O_3$)m/z$^+$(%): 604.50 $[M+1]^+$ (15); 605.47 $[M+2]^+$ (5); ^{1}H NMR(400MHz, DMSO-d_6, 25°C, TMS, δ):10.69 (s, 1H), 8.82 (s, 1H), 7.84(dd, 1H, J_1 = 3.6Hz, J_2 = 1.6Hz), 7.52(m, 2H), 7.01(dd, 2H, J_1 = 4.0Hz, J_2 = 2.4Hz), 6.91(d, 1H, J = 8.8Hz), 6.28(s, 2H), 6.14(q, 1H, J_1 = 4.0Hz, J_2 = 2.4Hz), 5.93(d, 2H, J = 2.4Hz), 5.03(t, 2H, J = 5.6Hz), 3.09(m, 8H), 1.84 (s, 6H), 1.18(t, 6H, J = 7.2Hz), 1.01(t, 6H,

J = 7.2Hz); ^{13}C NMR (100MHz, DMSO-d_6, 25°C, TMS, δ):162.7, 159.6, 152.8, 151.0, 150.9, 150.3, 147.8, 133.3, 131.9, 129.2, 128.6, 126.8, 123.7, 122.7, 118.2, 106.3, 104.5, 95.7, 65.5, 43.8, 37.4, 16.9, 14.1, 12.3 ; Anal. calcd. For $C_{37}H_{41}N_5O_3$ (M_w = 603.32), %: C, 73.61; H, 6.84; N, 11.60; found, %: C, 73.25; H, 6.95; N, 11.28; IR $\upsilon_{str.}$(C=O): 1707 cm^{-1} (KBr). CCDC No. to crystal structure of **2**: 1963358.

Synthesis **3**

The Fluorescein hydrazide (**FH**) was synthesized from fluorescein(**F**) following a literature procedure[RS7], except that we have used EtOH as solvent instead of methanol as reported. The characterization of synthesized **FH** matched well to reported values, and used subsequently.

To a stirring solution of **FH**(0.346g, 1.0mmol) in EtOH(15mL), trans-4-(diethyl amino)-cinnamaldehyde (0.203g, 1.0mmol) in EtOH(15mL) was added drop wise followed by addition of glacial acetic acid(catalytic amount) and heated to reflux for 6h with constant stirring until a yellow colourization of the solution was observed. The reaction mixture was filtered while hot and the solvent was allowed to evaporate at room temperature, where upon the desired product **3** were precipitated as yellow coloured single crystals, suitable for X-ray diffraction through slow evaporation technique.

3. Yield: 0.40g(76%); m. p. = 185 °C; ESI-MS($C_{33}H_{29}N_3O_4$) m/z$^+$(%): 532[M+1]$^+$ (100); 533[M+2]$^+$ (48), 554[M+3]$^+$(8); ^{1}H NMR (400 MHz, DMSO-d_6, 25°C, TMS, δ): 9.87(s, 2H), 8.84(d, 1H, J = 9.5Hz) 7.84(d, 1H, J= 6.5Hz), 7.53(m, 2H), 7.33(d, 2H, J = 8.5Hz), 7.00 (dd, 1H, J_1 = 2.0Hz, J_2 = 1.5Hz), 6.75(d, 1H, J=5.5Hz), 6.61(d, 2H, J = 2.0Hz), 6.56(d, 2H, J = 9.0Hz), 6.46(m, 5H), 3.31(q, 4H, J = 7.0Hz), 1.04(m, 6H), ^{13}C NMR (100 MHz, DMSO-d_6, 25°C, TMS, δ):164.0, 158.9, 155.5, 152.3, 151.6, 148.6, 142.1, 134.0, 129.6, 129.3, 129.2, 128.5,123.9, 123.4, 122.9, 120.6, 112.8, 11.6, 110.7, 103.0, 65.5, 56.54, 12.9.

CCDC No. to crystal structure of **3**: 1978815.

References:

RS1. M. Fischer and J. Georges, *Chem. Phys. Lett.,* 1996, **260**, 115.

RS2. S. Uchiyama, Y. Matsumura, A. P. de Silva and K. Iwai, *Anal. Chem*., 2003, **75**, 5926.

RS3. (a) C. R. Lohani, J. -M. Kim, S.-Y. Chung, J. Yoon and K. -H. Lee, *Analyst*, 2010, **135**, 2079; (b) Hans-Peter Loock and Peter D. Wentzell, *Sens. Actuat. B*, 2012, **173**, 157.

RS4. Q.-X. Liu, Z.-Q. Yao, X.-J. Zhao, Z.-X. Wang and X.-G. NHC *Organometallics,* 2013, **32**, 3493.

RS5. J. R. Lakowicz, Principles of Fluorescence Spectroscopy, 3rd edn., Springer Science, 2006, pp. 141-143.

RS6. (a) D. Wu, W. Huang, C. Duan, Z. Lin, and Q. Meng, *Inorg. Chem*., 2007, **46**, 1538; (b) Y.-K. Yang, K.-J. Yook, and J. Tae, *J. Am. Chem. Soc*., 2005, **127**, 16760

RS7. J. D. Villada, R. F. D'Vries, M. Macĩas, F. Zuluaga and M. N. Chaur, *New J. Chem.,* 2018, **42**, 18050.

Table ST1: Crystallographic parameters pertaining to structures of **1**, **2** and **3**

Parameters	**1**	**2**	**3**
Empirical formula	$C_{74}\ H_{85}\ N_{10}\ O_6$	$C_{37}\ H_{41}\ N_5\ O_3$	$C_{35}\ H_{35}\ N_3\ O_5$
Chemical formula	$2[(C_{37}H_{40}N_5O_2).(H_{1.5}O_1)]$	$C_{37}H_{41}N_5O_3$	$[C_{33}H_{29}N_3O_4).C_2H_5OH]$
Formula weight	1210.51	603.77	577.66
Temperature (K)	293(2)	293(2)	102(2)
Wavelength (Å)	0.71073	0.71073	0.71073
Crystal structure	Block	Block	Block
Crystal colour	Colourless	Colourless	Colourless
Crystal system	Monoclinic	Monoclinic	Monoclinic
Space group	P 2_1/c	P 2_1/c	C c
a, Å	9.309(2)	9.236(2)	16.2392(19)
b , Å	14.055(3)	14.416(3)	12.0245(16)
c, Å	25.600(6)	25.771(6)	17.250(2)
α, (°)	90.00	90.00	90.00
β, (°)	95.73(6)	95.167(7)	110.696(3)
γ, (°)	90.00	90.00	90.00
Volume, U ($Å^3$)	3332.7(3)	3417.6(14)	3151.0(7)
Z	2	4	4
Crystal Density (ρ, g/cm^3)	1.206	1.1733	1.218
Absorption coefficient(μ,mm^{-1})	0.078	0.076	0.082
F(000)	1294	1288.5	1224
Reflections collected	25247	15532	7413
Data	4782	2005	1882
Reflections (unique), [I>2σ(I)]	3531	1732	1824
Restraints	3	37	2
Parameters	544	467	400
Goodness of Fit (on F^2), S	1.027	1.1554	1.076
R(Final) R1=	0.0579	0.0570	0.0278
[I>2σ(I)] wR2=	0.1623	0.1550	0.0639
R (all data) R1=	0.0758	0.0639	0.0297
wR2=	0.1826	0.1610	0.0652

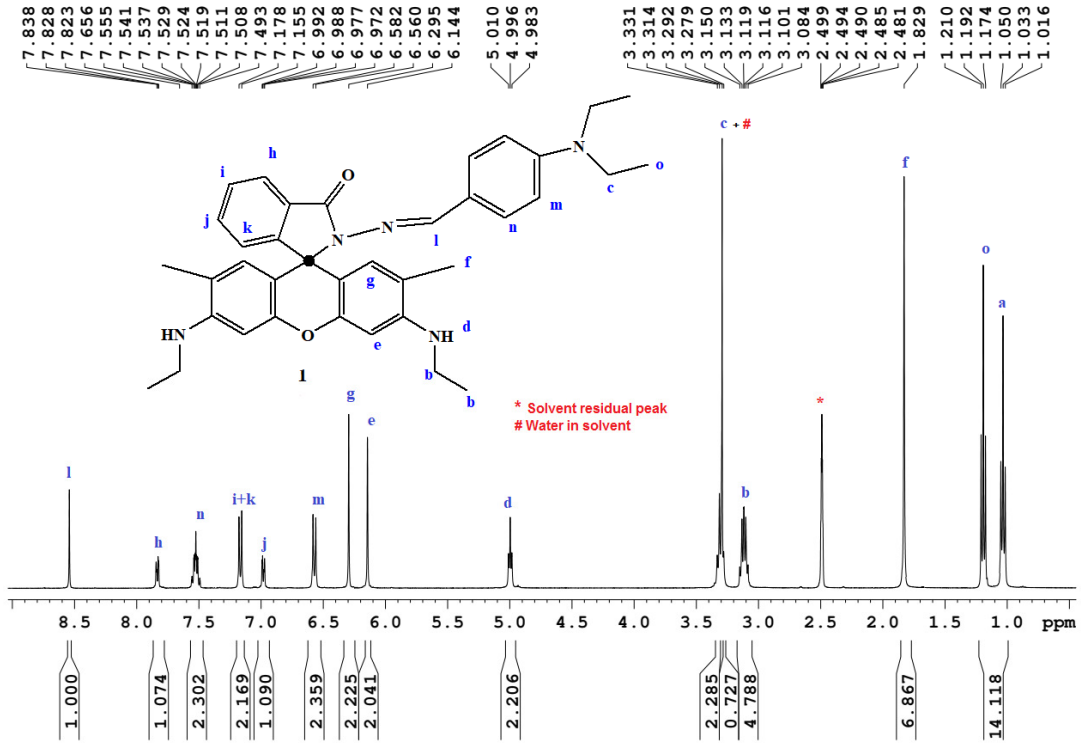

Fig. S1: ^{1}H-NMR spectrum of **1**(DMSO-d_6).

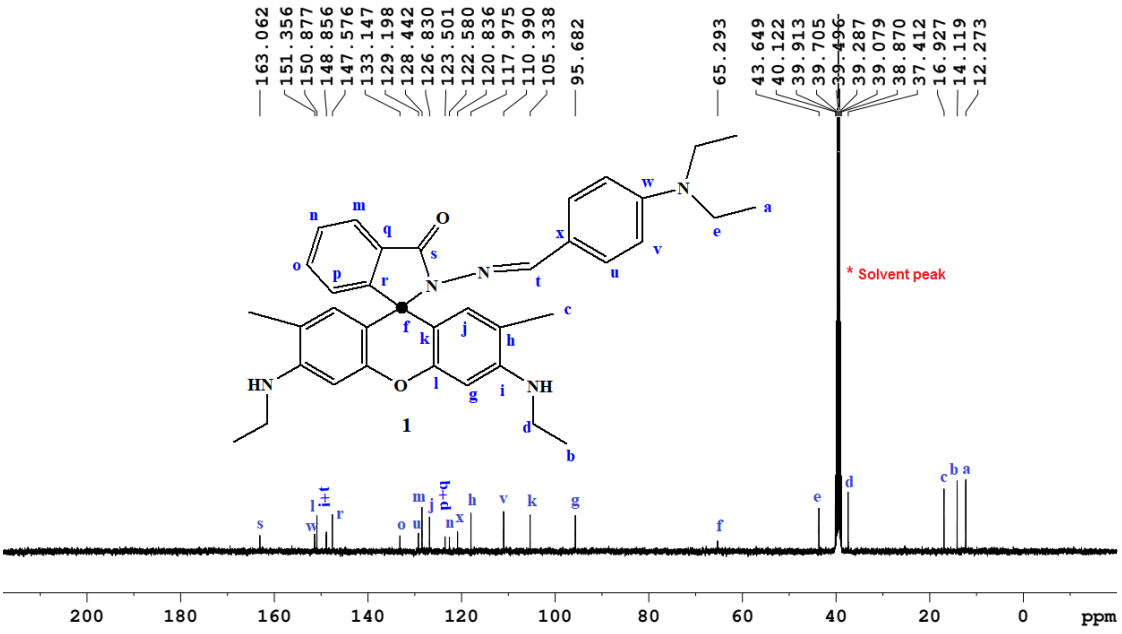

Fig. S2: ^{13}C-NMR spectrum of **1**(DMSO-d_6).

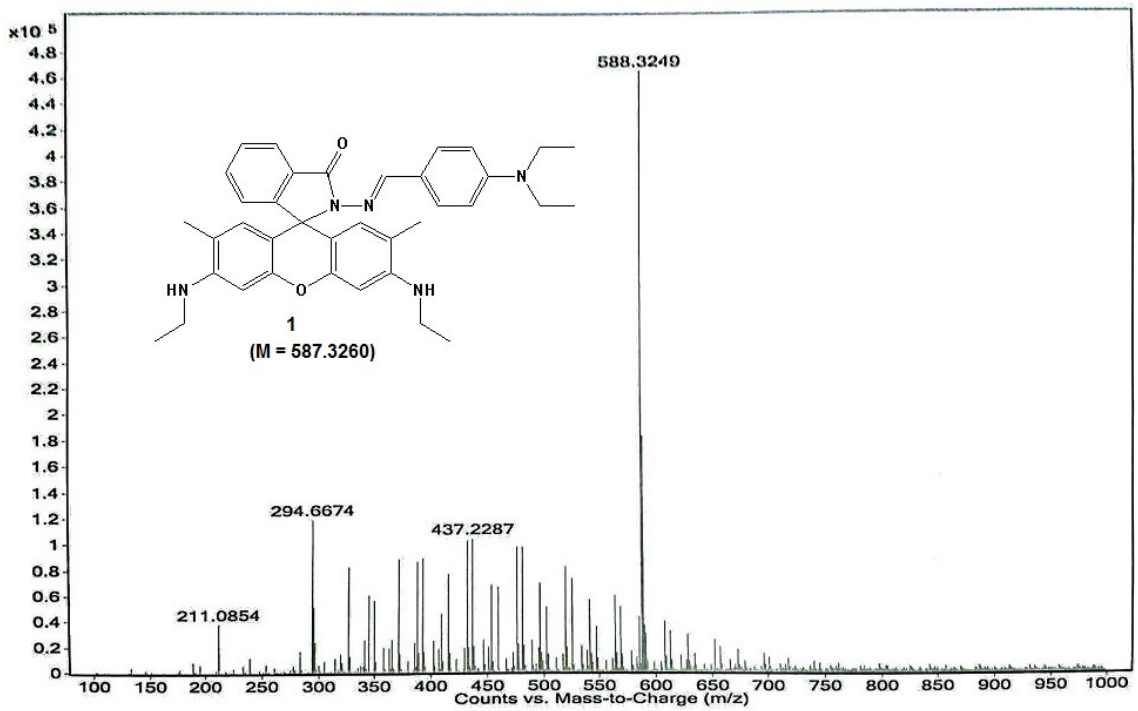

Fig. S3: MS (+ESI) spectrum of **1**.

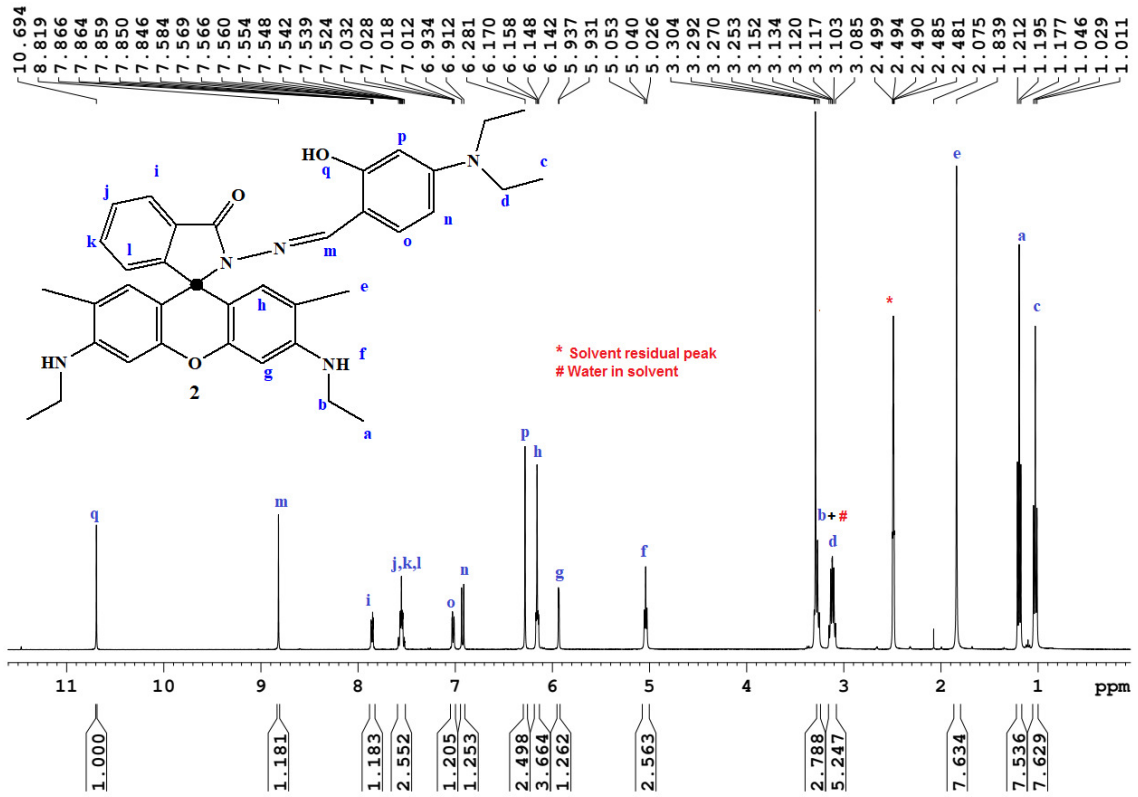

Fig. S4: ^{1}H-NMR spectrum of **2**(DMSO-d_6).

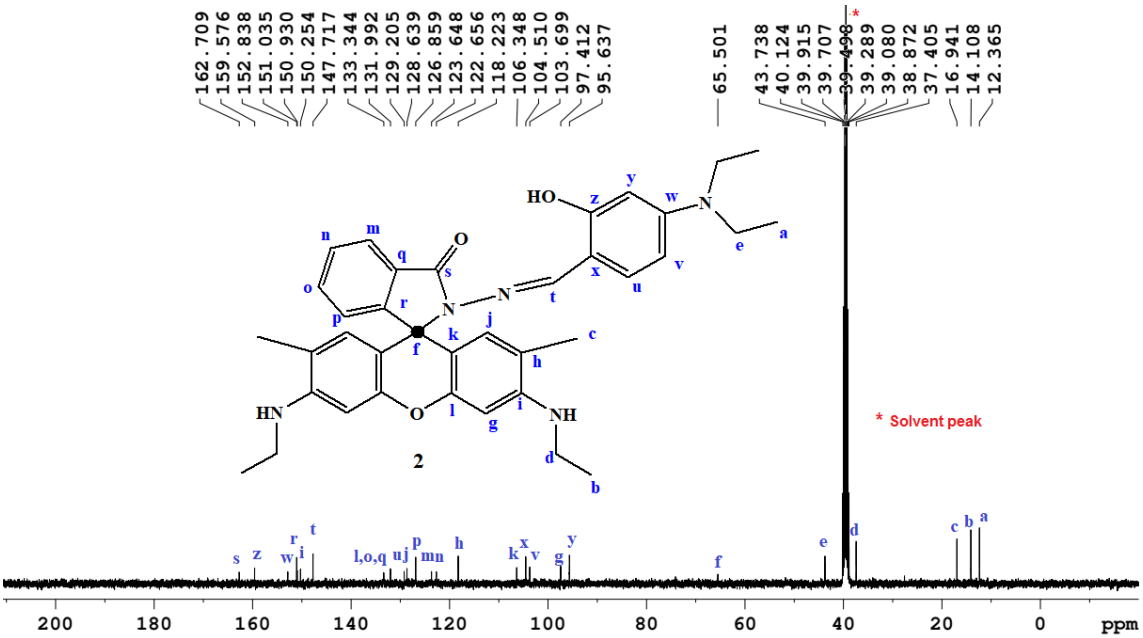

Fig. S5: ^{13}C-NMR spectrum of **2**(DMSO-d_6).

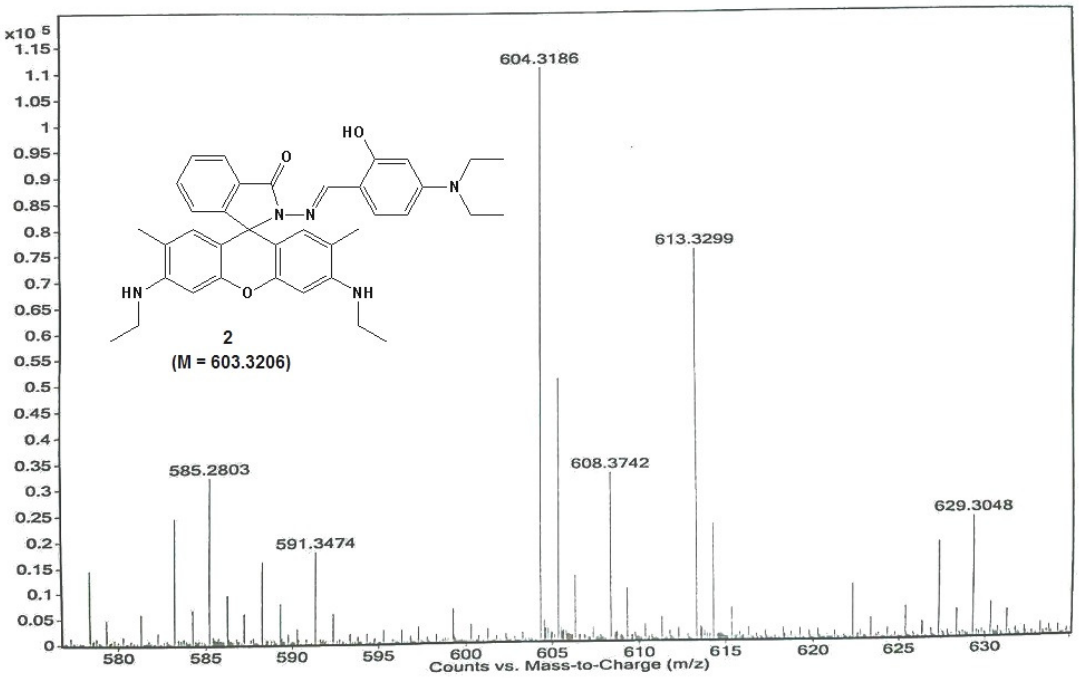

Fig. S6: MS (+ESI) spectrum of **2**.

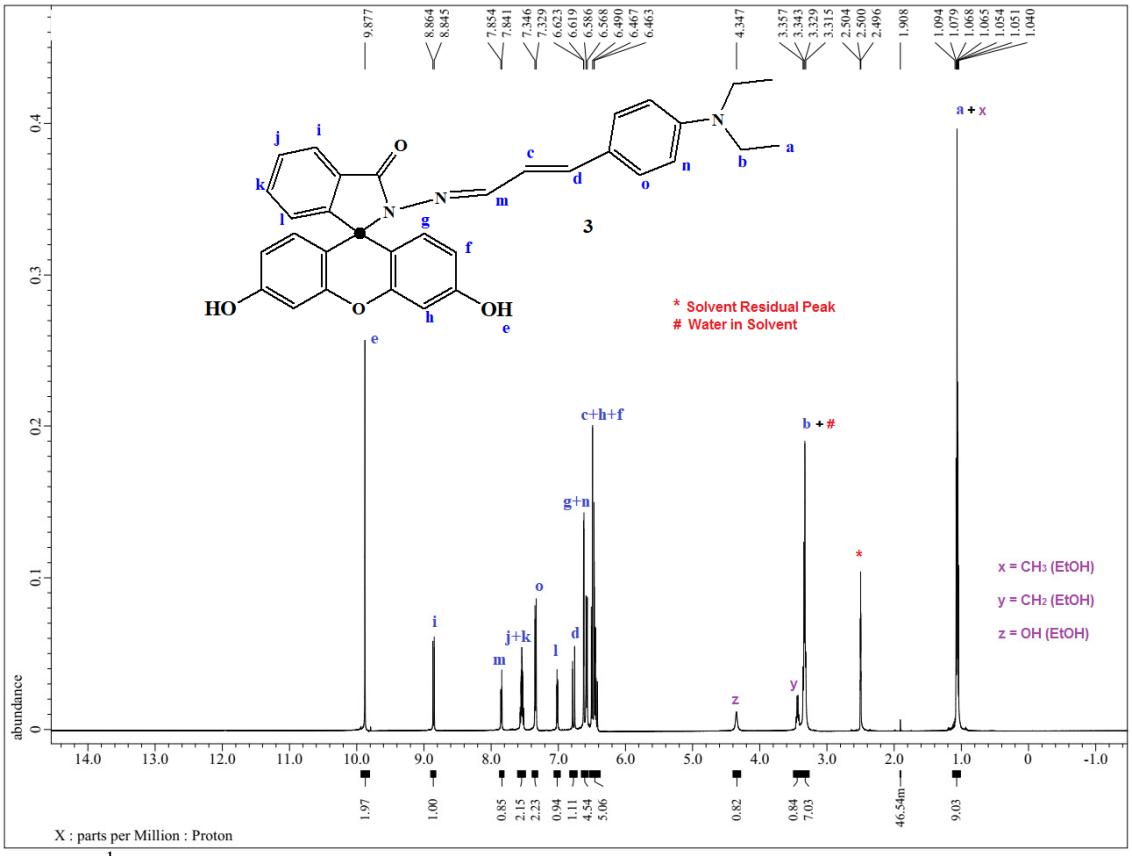

Fig. S7: ^{1}H-NMR spectrum of **3**(DMSO-d_6).

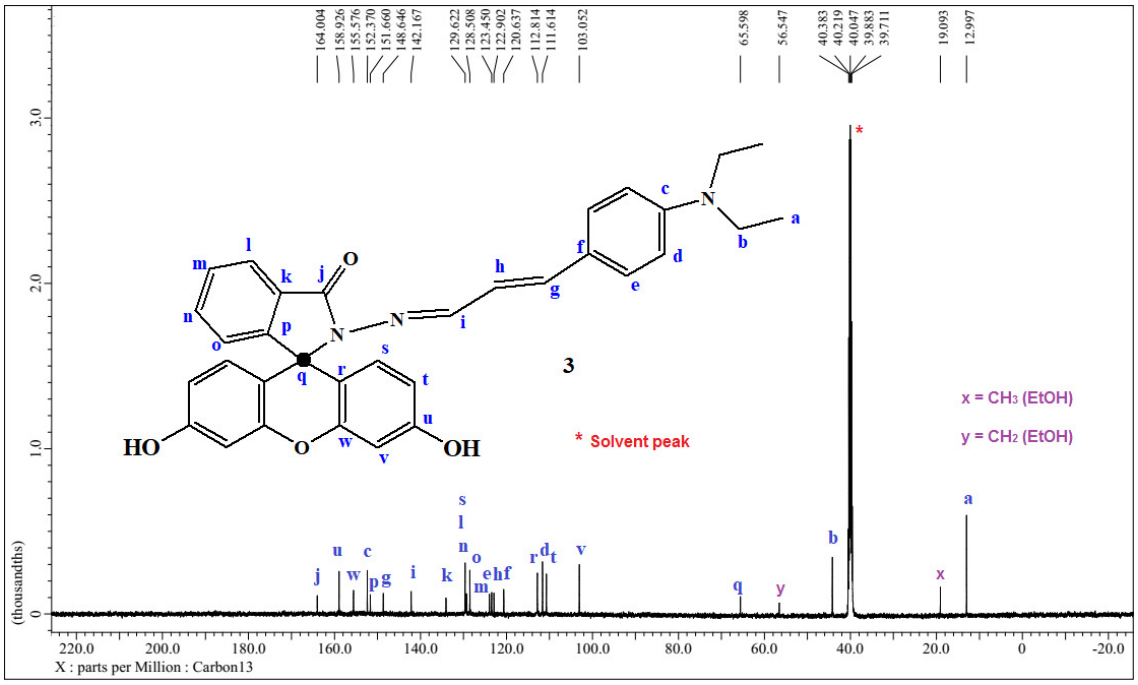

Fig. S8: ^{13}C-NMR spectrum of **3**(DMSO-d_6).

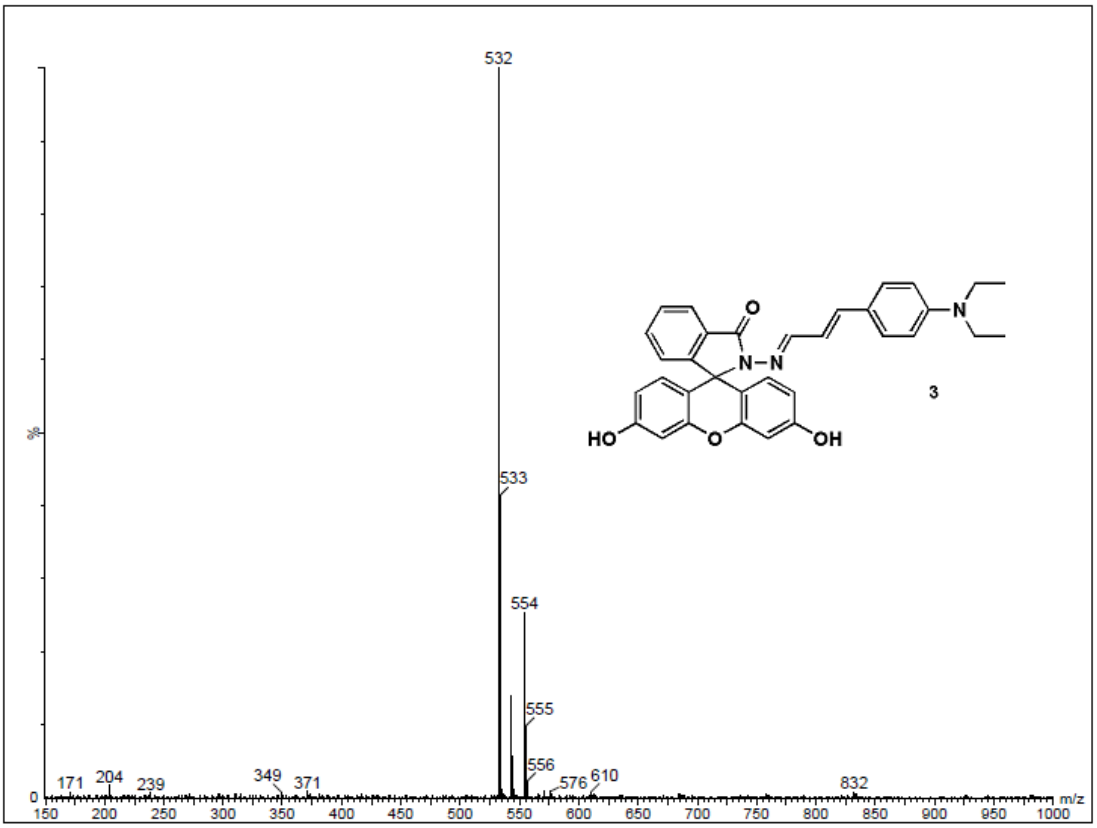

Fig. S9: ESI-MS spectrum of **3**.

Photophysical investigations

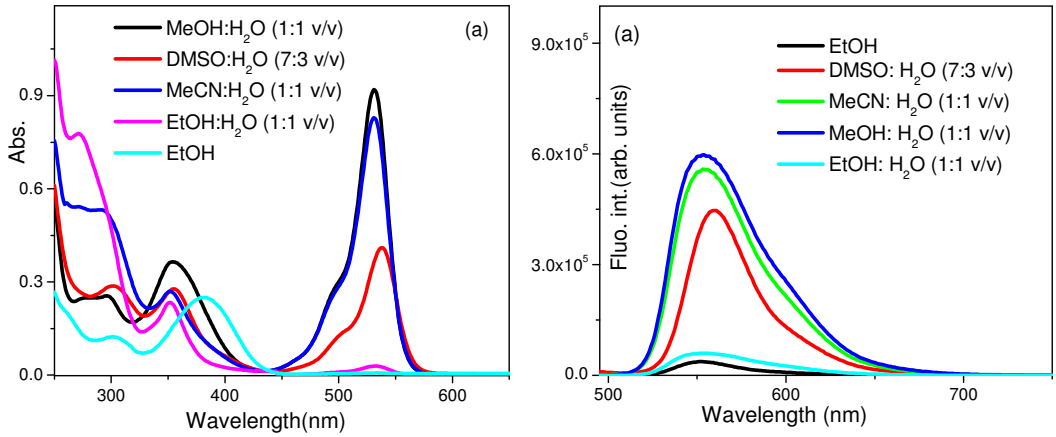

Fig. S10: (a) Absorption and (b) fluorescence spectra of **1** in various solvents. Abs: [**1**] = 1×10^{-4}M, Fluorescence: [**1**] =1μM, λ_{ex}=480nm, RT, ex. and em. b. p.=5nm.

The absorbance of **1** at 535(±5) nm in all these solvent conditions are <0.1 in its 10μM concentration (< 0.01 in EtOH-H_2O, 1:1 v/v). The absorption spectra were recorded at higher concentration (100μM) to show that **1** is susceptible to undergo partial solvent assisted spiro-ring opening, a phenomenon observed with rhodamine B based compounds in earlier reports (ref: B. Bag and A. Pal, *Org. Biomol. Chem.*, 2011, **9**, 915). The fluorescence quantum yield in all cases were calculated to be <0.001.

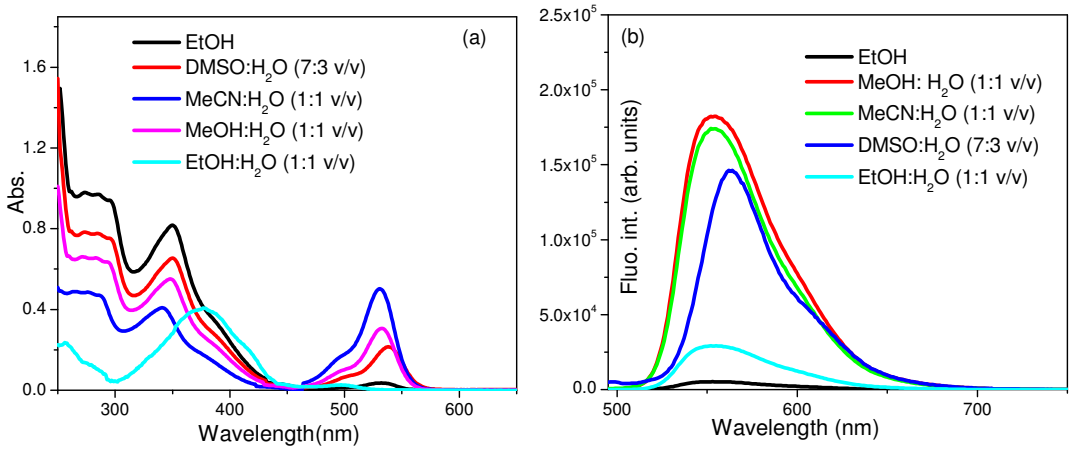

Fig. S11: (a) Absorption and (b) fluorescence spectra of **2** in various solvents. Abs: [**2**]= 1×10^{-4}M, Fluorescence: [**2**]=1μM, λ_{ex}=480nm, RT, ex. and em. b.p.=5nm.

Similar to those observed for **1**, the absorbance of **2** at 535(±5) nm in all these solvent conditions are <0.1 in its 10μM concentration (< 0.01 in EtOH-H_2O, 1:1 v/v). The absorption spectra were recorded at higher concentration (100μM) to show that **2** is susceptible to undergo partial solvent assisted spiro-ring opening. In all cases, the fluorescence quantum yield was found to be < 0.001.

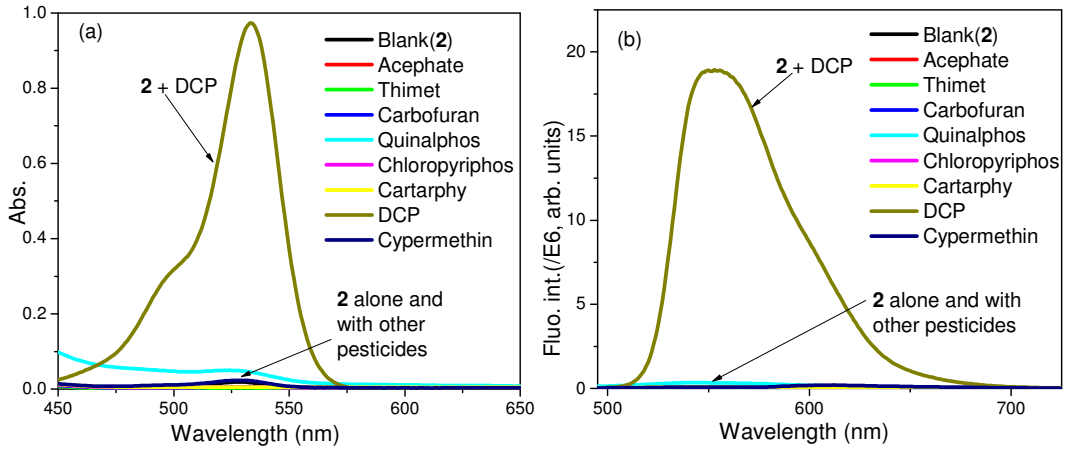

Fig. S12: (a) Absorption and (b) fluorescence spectra of **2** alone and in presence of various pesticides in EtOH-H_2O (1:1 v/v, 0.1M PBS, pH = 7.1) medium. Conditions: Absorption: [**2**] = 10 μM; Fluorescence: [**2**] = 1μM, RT, λ_{ex} = 480 nm, em. /ex. b. p.=5 nm.

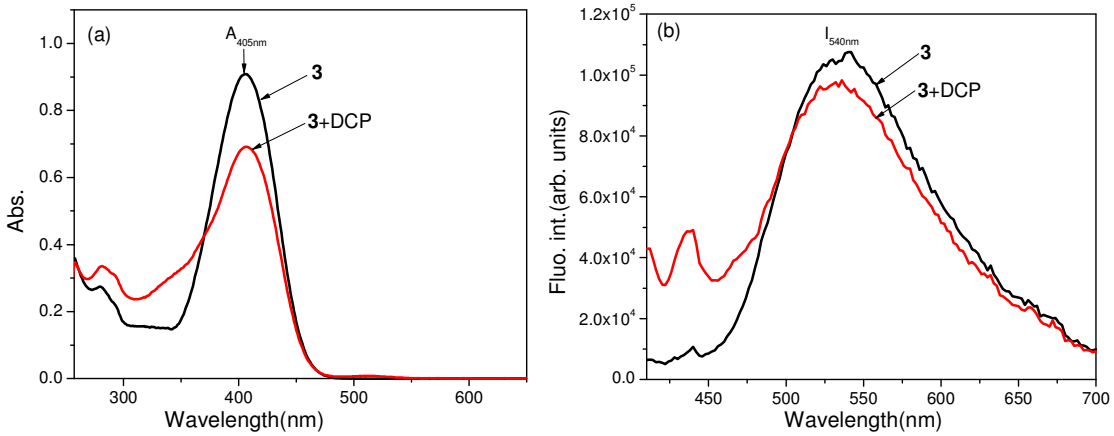

Fig. S13. (a) Absorption and (b) fluorescence spectra of **3** alone and in presence DCP in DMSO medium, Conditions: Absorption: [**3**] = 10 μM; Fluorescence: [**3**] = 1μM, RT, λ_{ex} = 400 nm, em. /ex. b. p.=5 nm.

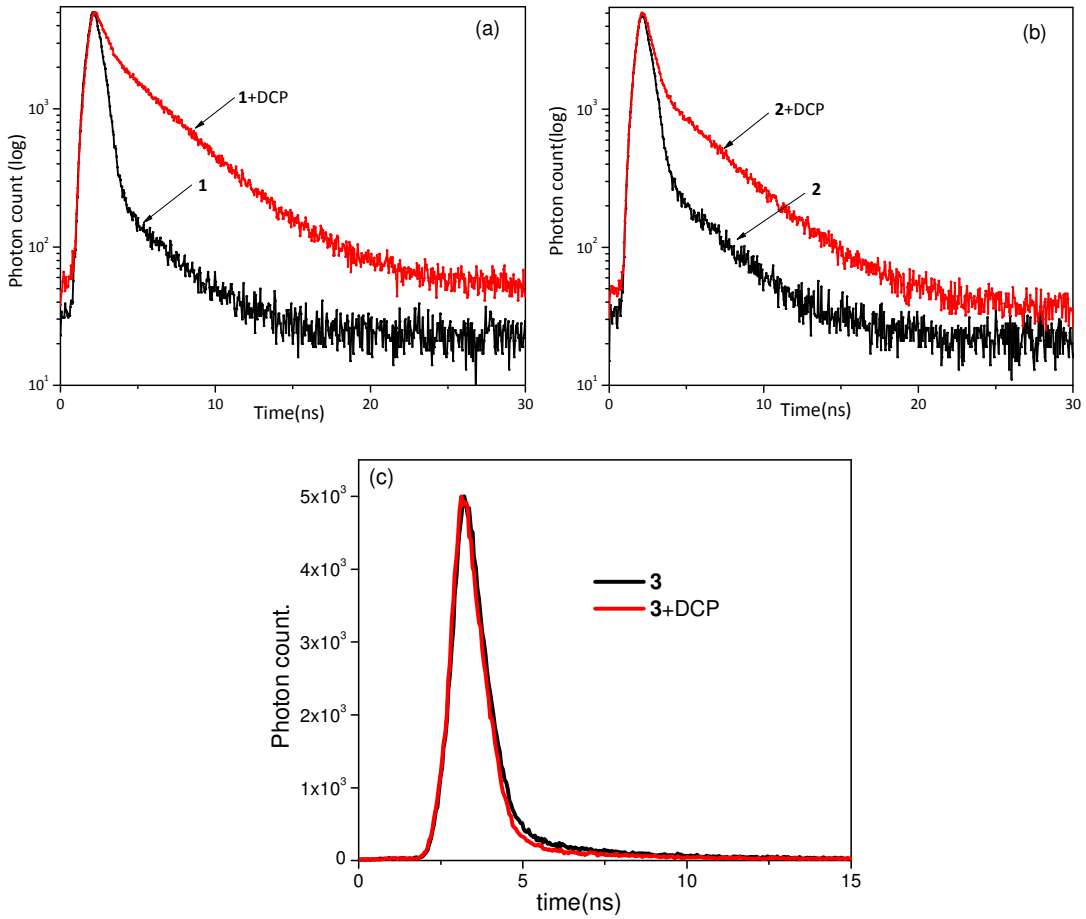

Fig. S14: The time-correlated single photon count (TCSPC) decay profile of the probes alone and with DCP in EtOH-H_2O (1:1 v/v, 0.1 M PBS, pH = 7.1) for (a) **1** and (b) **2** and in DMSO for (c) **3** (The excitation at 474nm and emission park at 540 nm using 470 nm laser). The average life-time was calculated from the bi-exponential fit equation to the decay profile.

Table ST 2: Fit-results to the exponential decay curve of **1**-**3** without and with DCP, which were obtained with time-correlated single photon counting technique with exponential fit equation $A+B_1 \exp(-t/\tau_1) + B_2 \exp(-t/\tau_2)$

Parameter	**1**	**1**+DCP	**2**	**2**+DCP	**3**	**3**+DCP
τ_1, ns (%)	0.37 (49.15)	0.36 (3.27)	0.42 (50.60)	0.49 (19.97)	0.49	0.47
τ_2, ns (%)	3.70 (50.86)	3.82 (96.73)	3.63 (49.40)	3.96 (80.03)	3.23	3.28
τ_{av}, ns	2.06	3.71	2.01	3.23	1.59	1.21
B1	2058.625	924.807	2875.652	3047.234	3194.92	3621.64
B2	212.979	2589.264	325.914	1524.168	326.28	186.159
A	19.795	49.710	19.767	31.652	19.13	18.730
χ^2	1.132	1.022	1.158	1.130	1.273	1.429

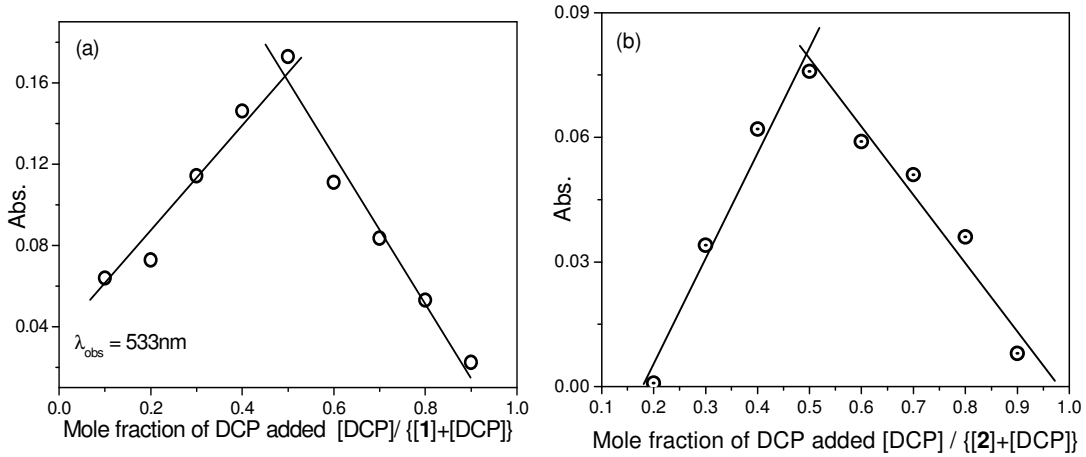

Fig. S15: Plot of absorbance (λ_{obs}= 533nm) of (a) **1** and (b) **2** against mole fraction of DCP added in EtOH-H_2O (1:1 v/v, 0.1M PBS, pH = 7.1) showing their 1:1 stoichiometry in in-situ adduct formation.

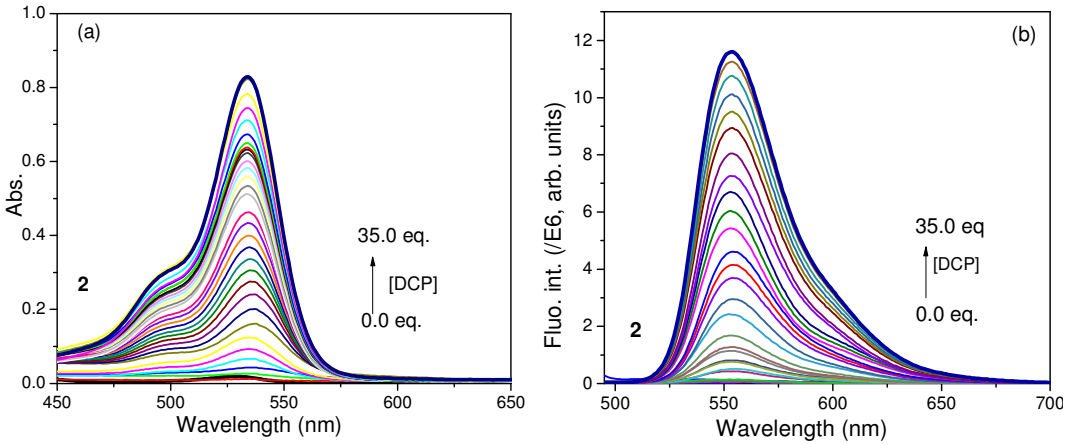

Fig. S16: (a) absorbance and (b) fluorescence spectra of **2** as a function of added DCP in EtOH–H_2O (1:1 v/v, 0.1M PBS, pH7.1). Abs.:[**1**] = 10 μM; Flu.: [**1**] = 1 μM, λ_{ex} = 480 nm, ex./em. band pass 5nm, RT.

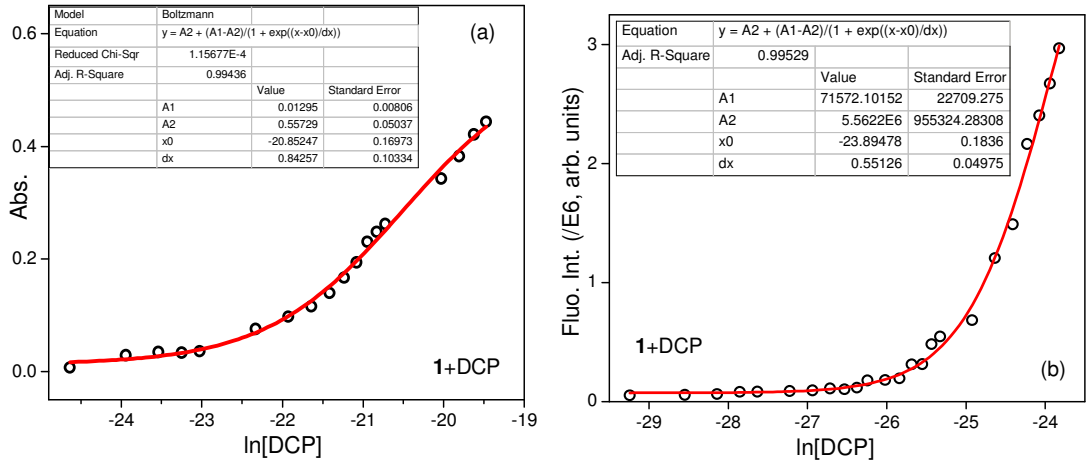

Fig. S17: Non-linear regression to the plot of (a) absorption(A_{533}) and (b) fluorescence (I_{553}) intensity of **1** in EtOH–H_2O (1:1 v/v, 0.1M PBS, pH7.1) as a function of concentration of DCP (ln DCP) for determination of association constant (Ka) through titration.

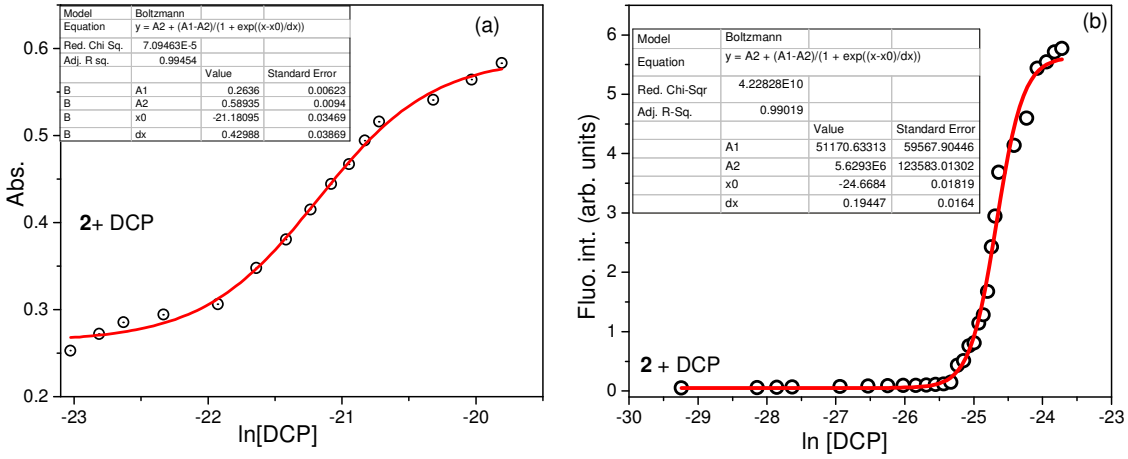

Fig. S18: Non-linear regression to the plot of (a) absorption(A_{533}) and (b) fluorescence (I_{553}) intensity of **2** in EtOH–H_2O (1:1 v/v, 0.1M PBS, pH7.1) as a function of concentration of DCP (ln DCP) for determination of association constant (Ka) through titration.

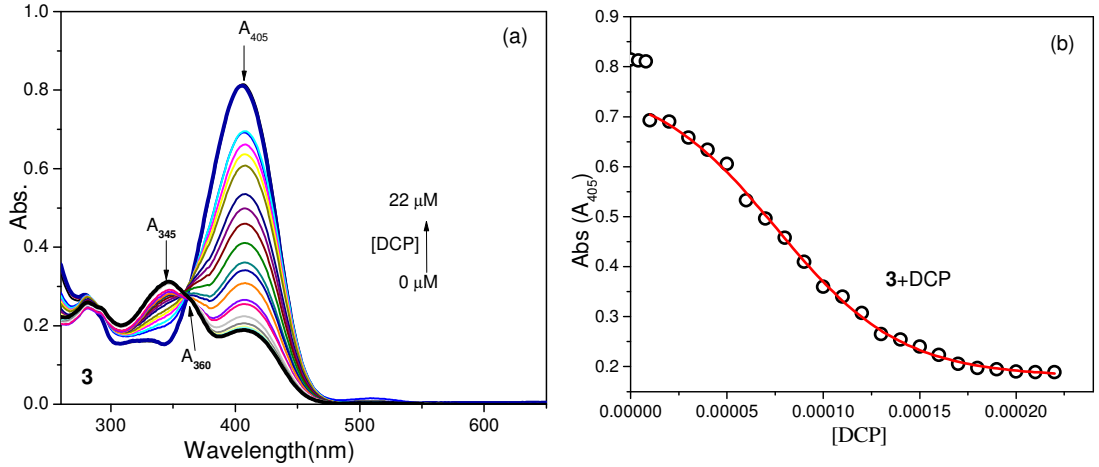

Fig. S19: (a) Absorbance spectra of **3** in DMSO and (b) its corresponding spectral profile at 405nm on gradual addition of DCP. [**3**] = 10 μM.

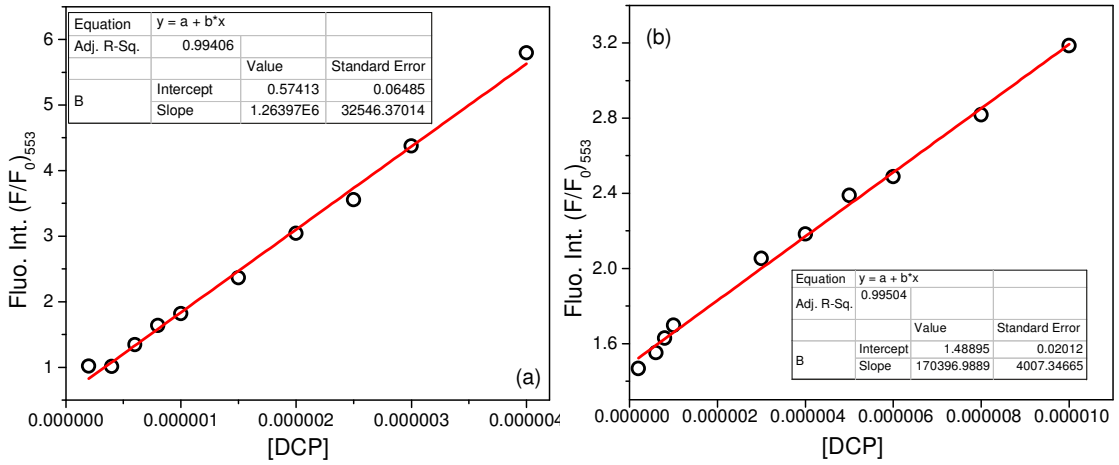

Fig. S20: Linear regressions of the plot of fluorescence spectral intensities[$(F/F_0)_{553}$] of (a) **1** (b) **2** with DCP at lower concentration level for determination of sensitivity of detection (S/N = 5).*Conditions*, Fluo.: [**1**]=[**2**]=1μM, RT, λ_{ex} = 480 nm, em. /ex. b. p.=5 nm.

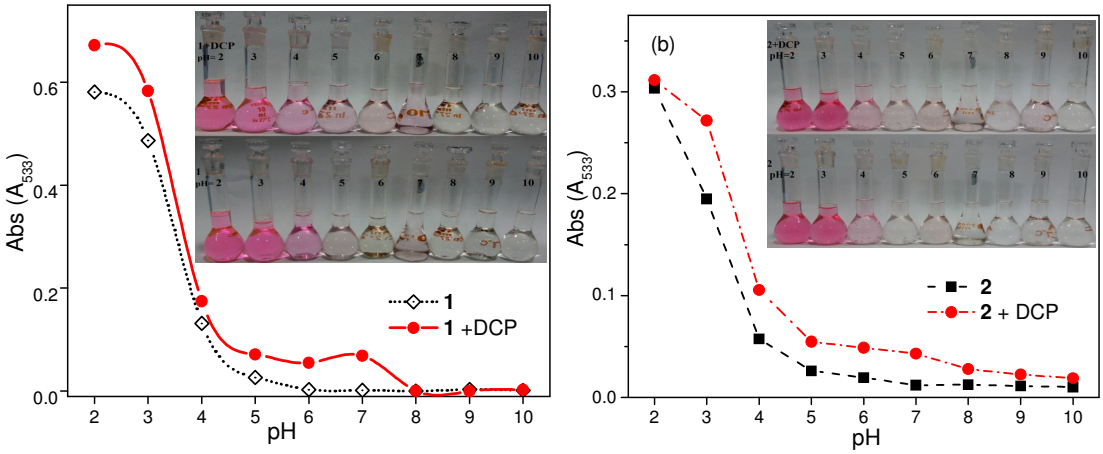

Fig. S21. Absorbance of (a) **1** and (b) **2** alone and in the presence of DCP in 2-10 pH. (Inset, a and b): Corresponding photographs of **1** and **2** respectively showing the colour change at varied pH. Experimental conditions: [**1**]=[**2**]=5 μM.

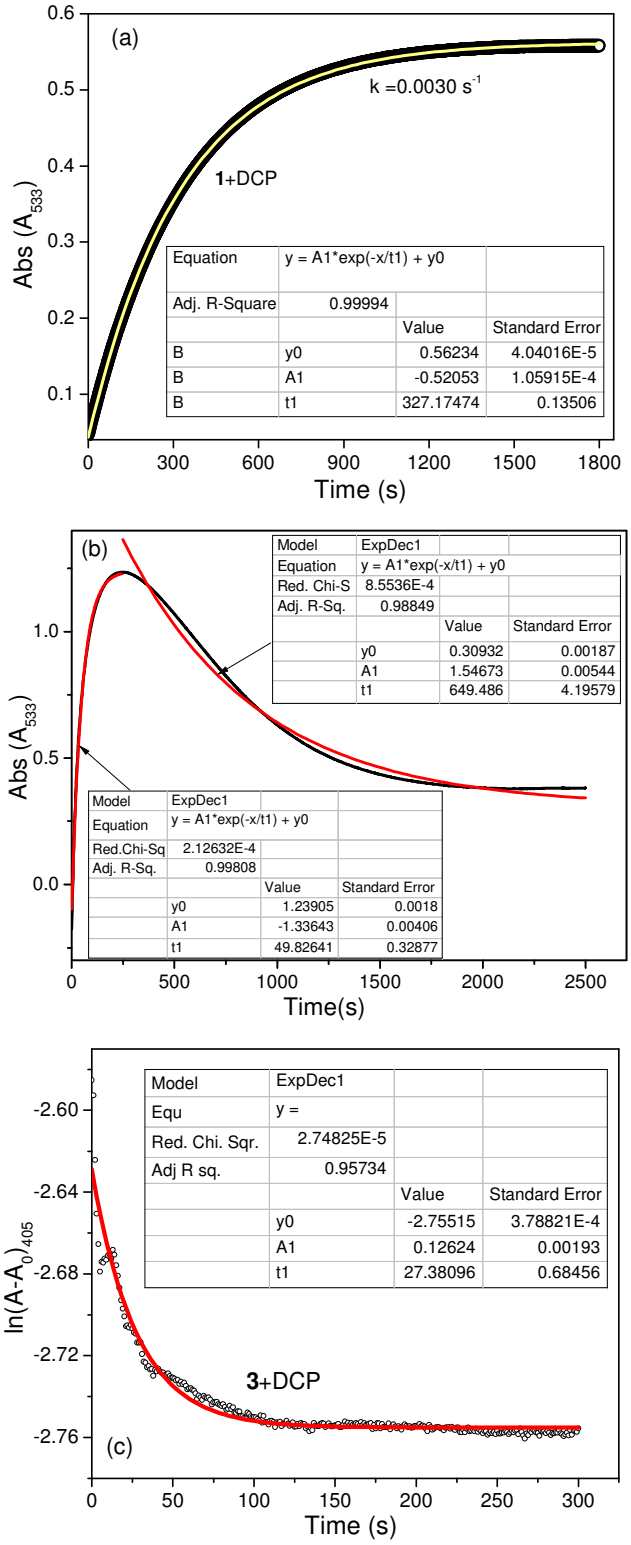

Fig. S22: Change in absorption in (a)**1**, (b) **2** and (c) **3** on addition of DCP as a function of time (s) in 1:1 (probe: DCP) stoichiometry. λ_{obs} = 533nm (**1** and **2**) and 405nm (for **3**). The non-linear regression fit ($A = A_0\, e^{-kt)}$) of first-order kinetics at the required time interval determines of rate constant (k) of the probe-adduct formation.

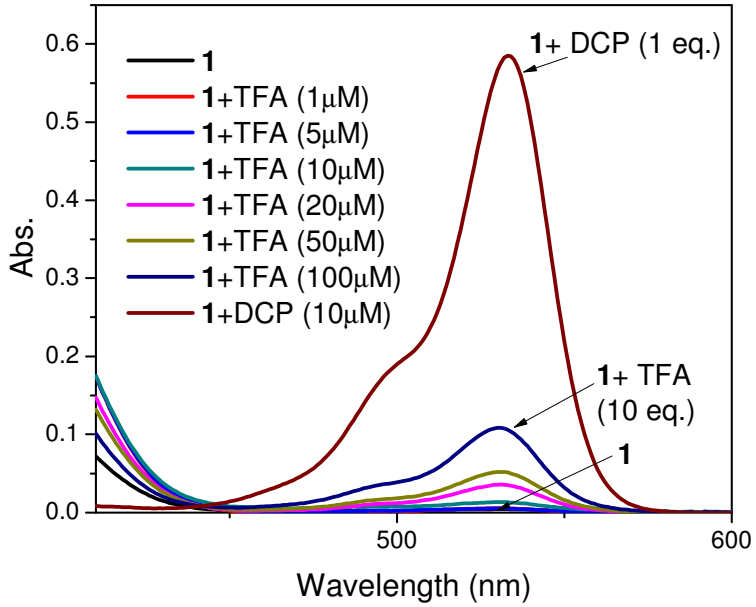

Fig. S23: Absorption spectra of **1** alone and in presence of Trifluoroacetic acid (TFA) in EtOH-H_2O (1:1 v/v, 0.1M PBS, pH = 7.1) medium. [**1**] = 10 μM. The absorption with **1**+DCP is shown for comparison. Although addition of TFA leads to spiro-ring opening, the absorbance for **1**+DCP (10μM) is much higher than **1**+TFA (100μM).

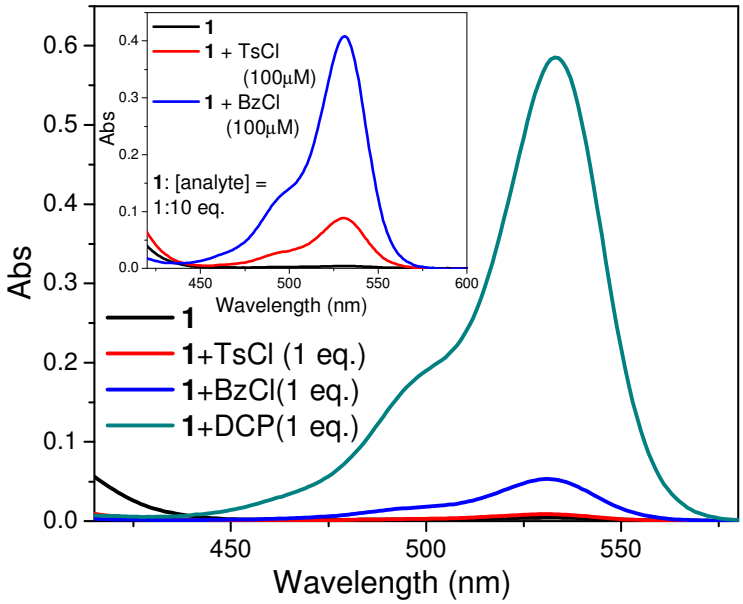

Fig. S24: Absorption spectra of **1**(10μM) on individual addition of equimolar of Tosyl chloride (TsCl), Benzoyl chloride (BzCl) and DCP in EtOH-H_2O (1:1 v/v, 0.1M PBS, pH = 7.1) medium. Inset: Absorption spectral enhancement in **1** on addition of TsCl (100μM) and BzCl(100μM) inferring the probe's spiro-ring opening by these analytes, yet to a lesser extent in comparison to that on addition of DCP.

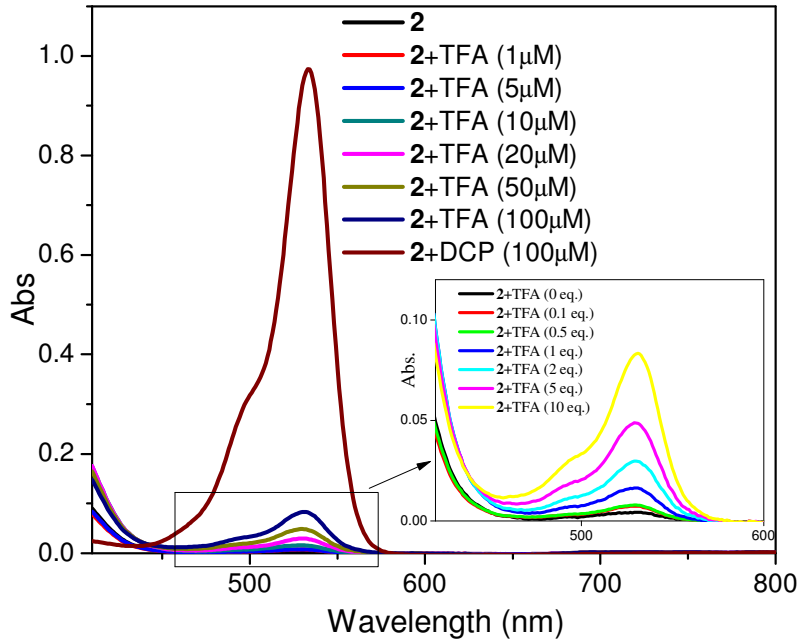

Fig. S25: Absorption spectra of **2** alone and in presence of Trifluoroacetic acid (TFA) in EtOH-H_2O (1:1 v/v, 0.1M PBS, pH = 7.1) medium. [**2**] = 10μM. The absorption with **2**+DCP(100μM) is shown for comparison. Although addition of TFA leads to spiro-ring opening, the absorbance for **2**+TFA (100μM) is much lower than **2**+DCP (100μM).

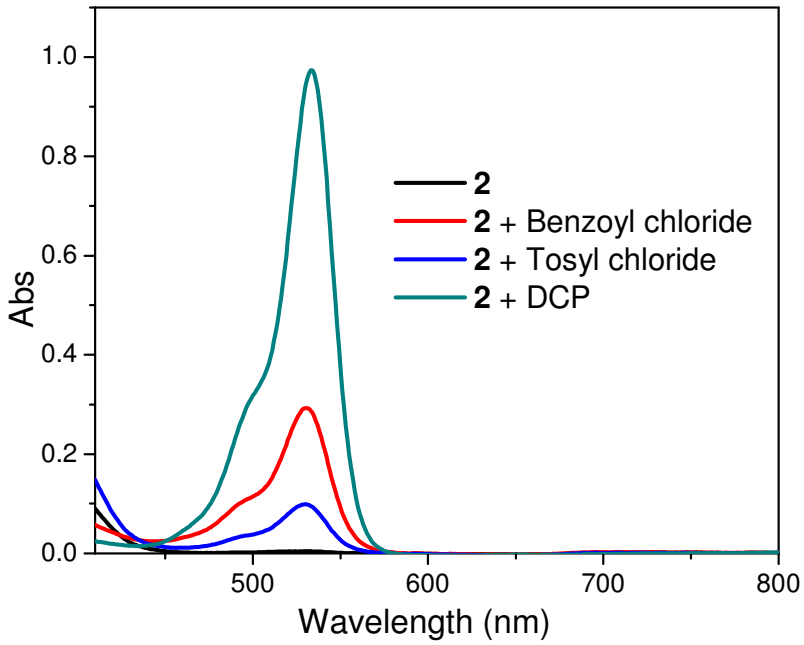

Fig. S26: Absorption spectra of **2**(10μM) on individual addition of equimolar of Tosyl chloride, Benzoyl chloride and DCP in EtOH-H_2O (1:1 v/v, 0.1M PBS, pH = 7.1) medium. The spiro-ring opening mediated absorbance responses on addition of tosyl chloride and benzoyl chloride is significantly lower in comparison to that on addition of DCP.

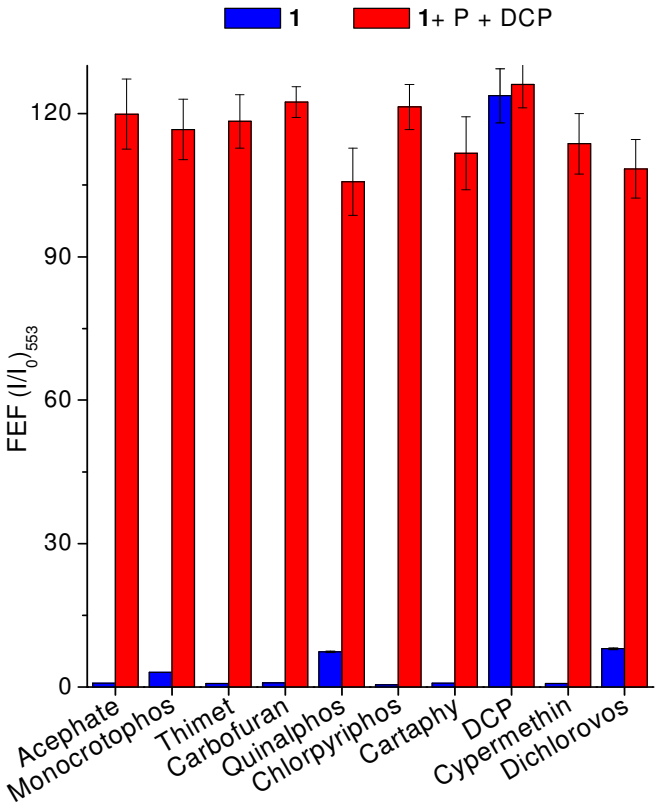

Fig. S27: The bar diagram to the corresponding fluorescence enhancement factors (at 553nm) of **1** with pesticides used in this study (blue coloured bar); subsequent addition of DCP to the solution containing **1** and individual pesticides, Conditions: λ_{ex} = 500nm, EtOH–H_2O (1:1 v/v, 0.1M PBS, pH7.1), [**1**] = 1μM, [Pesticides] = 20μM, ex. and em. b. p. = 5nm, RT.

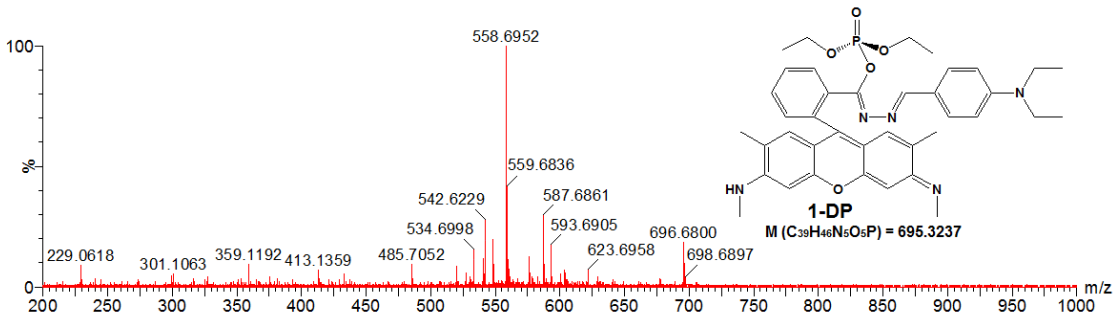

Fig. S28: ESI-MS spectra of in-situ **1**-DP adduct.

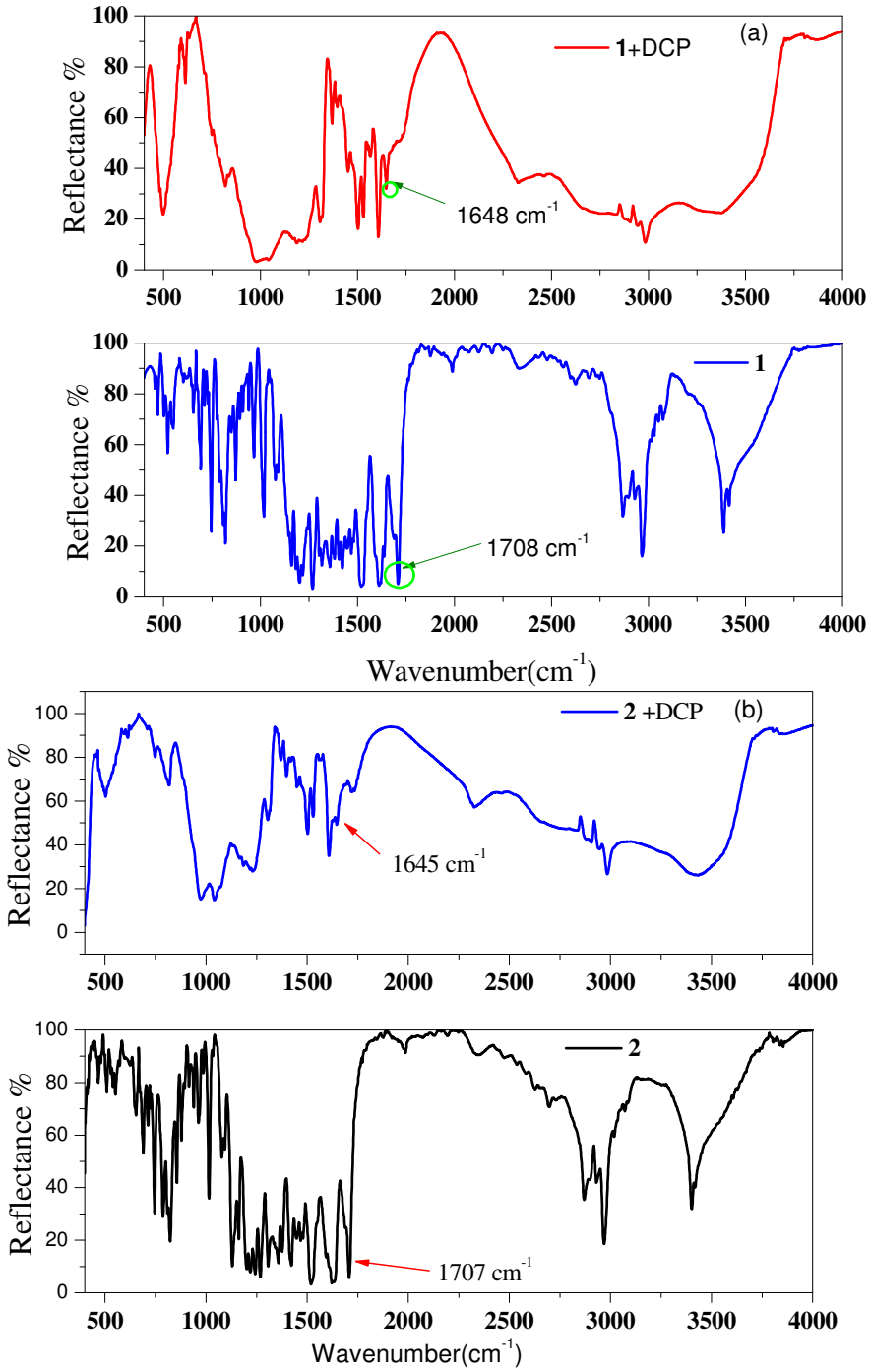

Fig. S29: FTIR spectrum of complexes of (a) **1** and (b) **2** alone and with DCP.

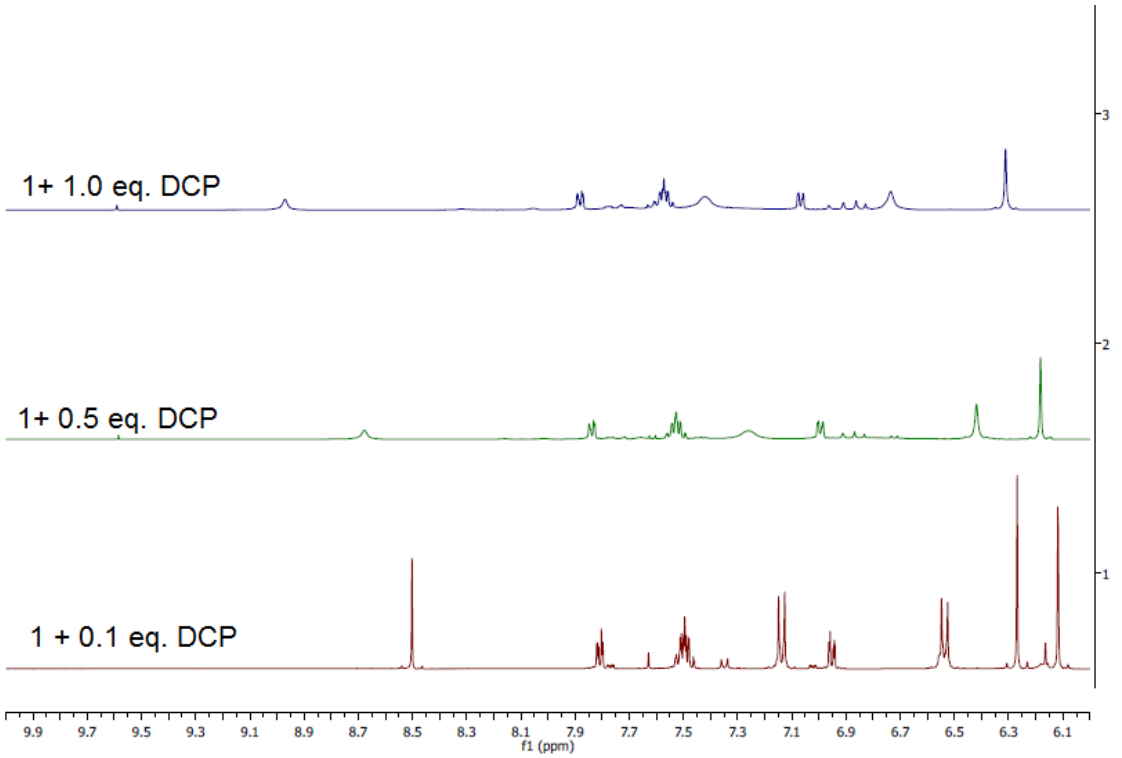

Fig. S30. ^{1}H NMR of **1**(20mM, DMSO-d_6, 400 MHz) in presence of DCP.

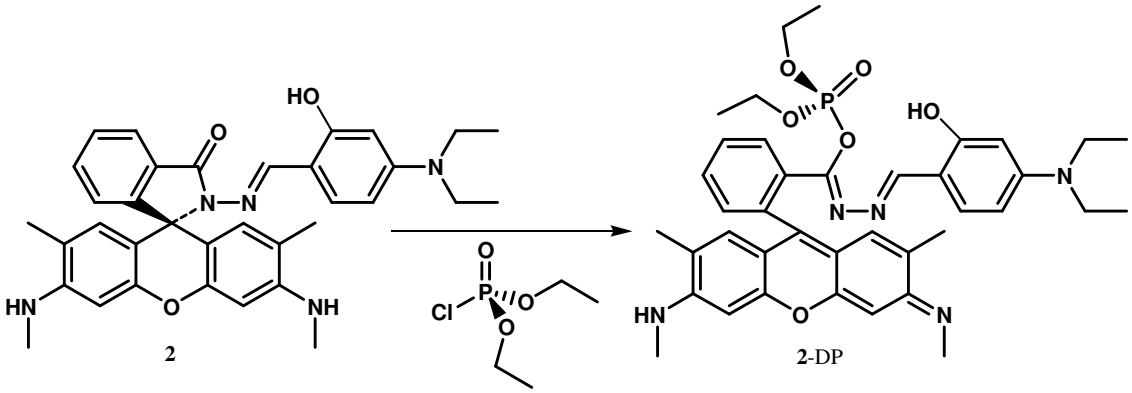

Scheme S3: The schematic representation of **2**-DP formation of **2**, which could translated to photophysical signalling in its DCP detection. The observed photophysical behaviour of **2** in presence of DCP is similar to that of **1**. One of the major concerns in **2** is the DCP-induced absorption spectral profile as a function of time, which argues for an interesting yet different mechanistic scenario of its formation. A further investigation would substantiate the mechanism, dynamics and behaviour of reaction. Nevertheless, extrapolation of phosphorylation mechanism in **1** allows the proposed binding mode in **2**-DP adduct formation, despite of an –OH binding site in its receptor, through a P–O linkage of electrophilic phosphorylation preferred at the spirocyclic $O_{carbonyl}$ site.

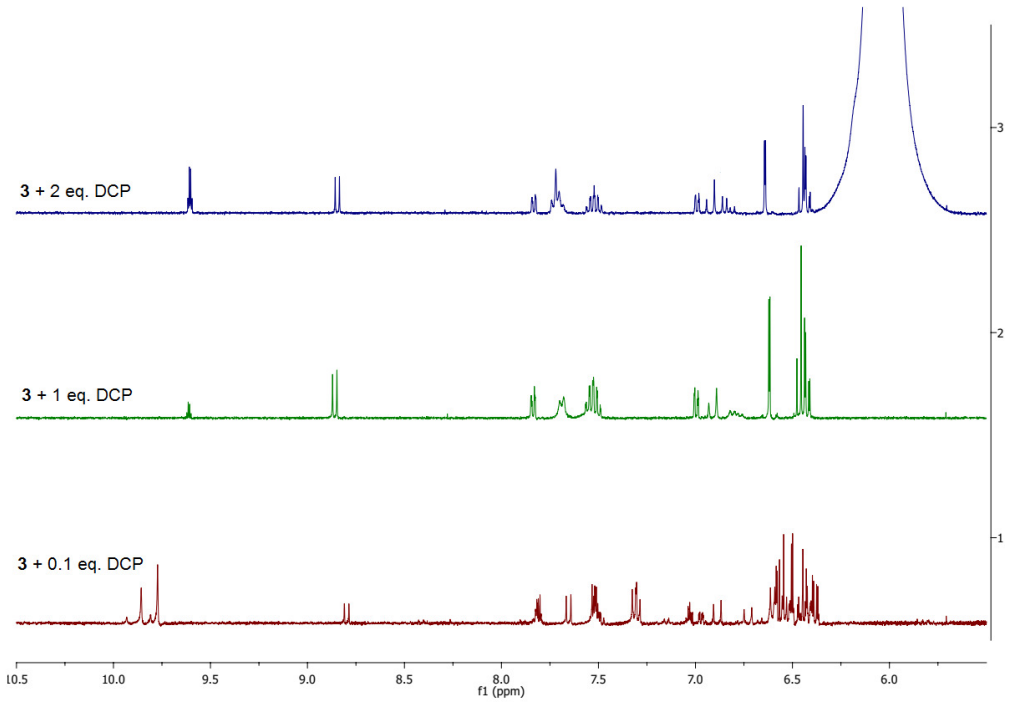

Fig. S31. ^{1}H NMR of **3** (10mM, DMSO-d_6) on addition of DCP.

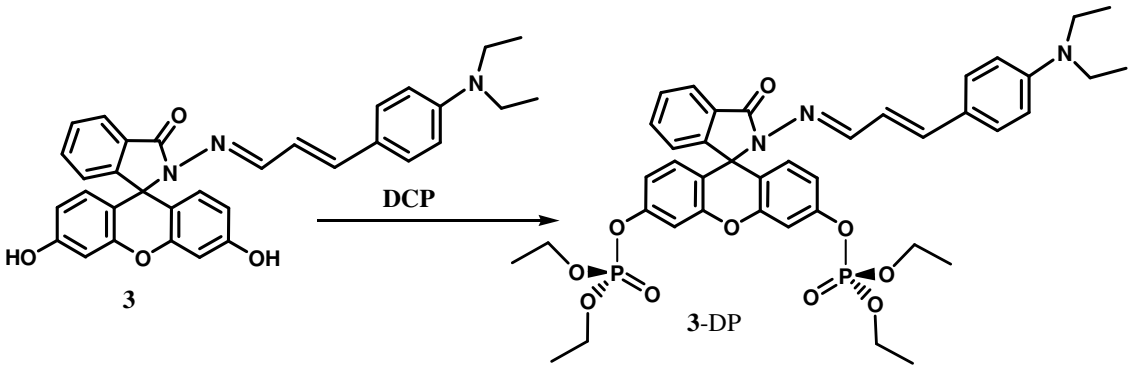

Scheme S4: Schematic representation of **3**-DP formation by **3** and DCP. Similar P–O linkage through electrophilic phosphorylation at –OH of the xanthene core of fluorescein is known.

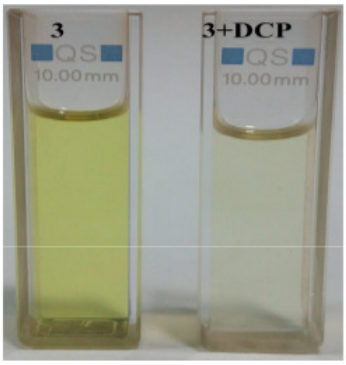

Fig. S32: Photograph of solution of **3**(10 μM) in DMSO alone and on addition of DCP.

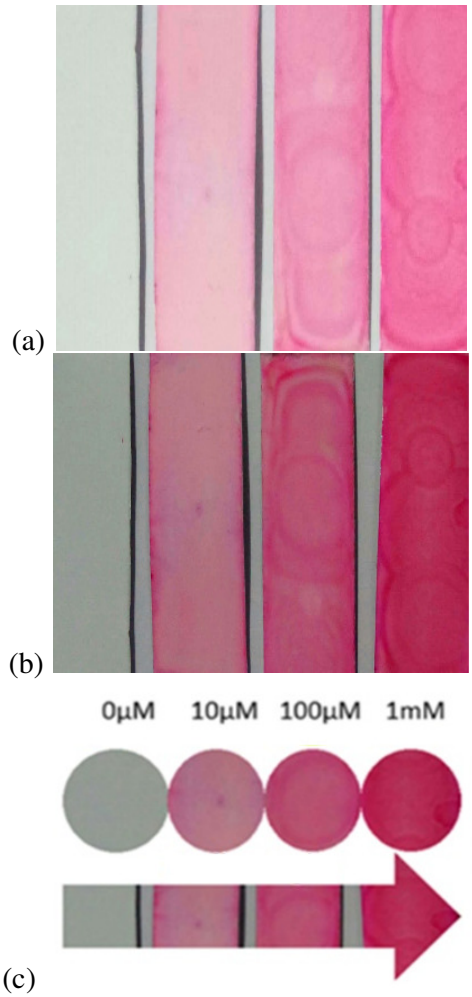

Fig. S33. The photographs of TLC plates showing colour change of (a) **1** and (b) **2** in visual detection of DCP vapours from its solution in (c) 0µM, 10µM, 100µM, 1mM concentration respectively. The methodology is described in experimental section.

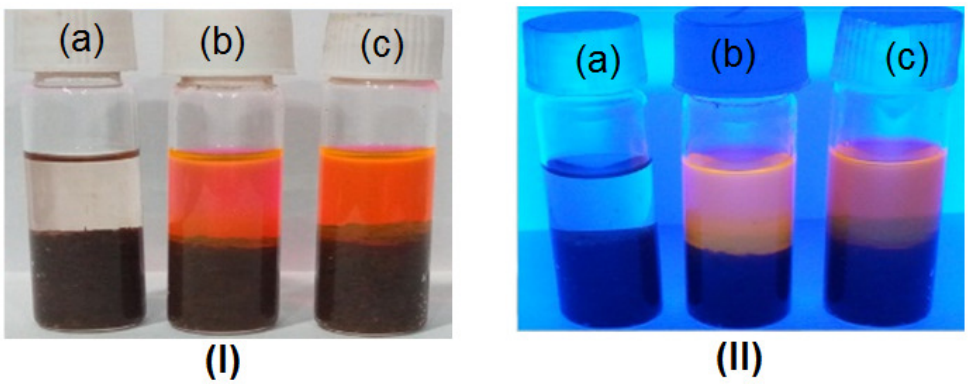

Fig. S34. The photographs of soil samples moistened with (a) DCP(10µM), dried and subsequent addition of aqueous-ethanolic (b) 1 or (c) 2 to the suspension showing colour change (chromogenic detection). (I) bare eye detection, (II) under UV-light illumination. The methodology is described in experimental section.

***Theoretical (DFT) calculations*:**

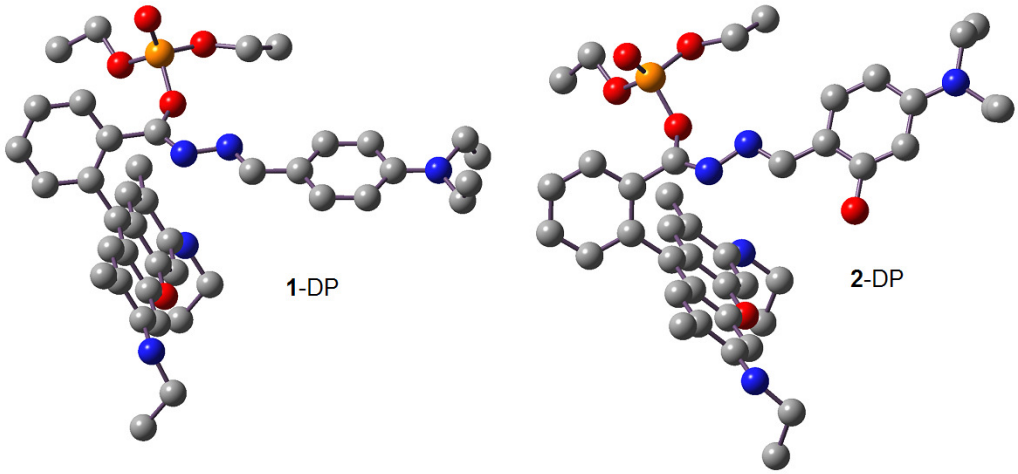

Fig. S35: Optimized structure of **1**-DP and **2**-DP. The H-atoms are omitted for clarity.

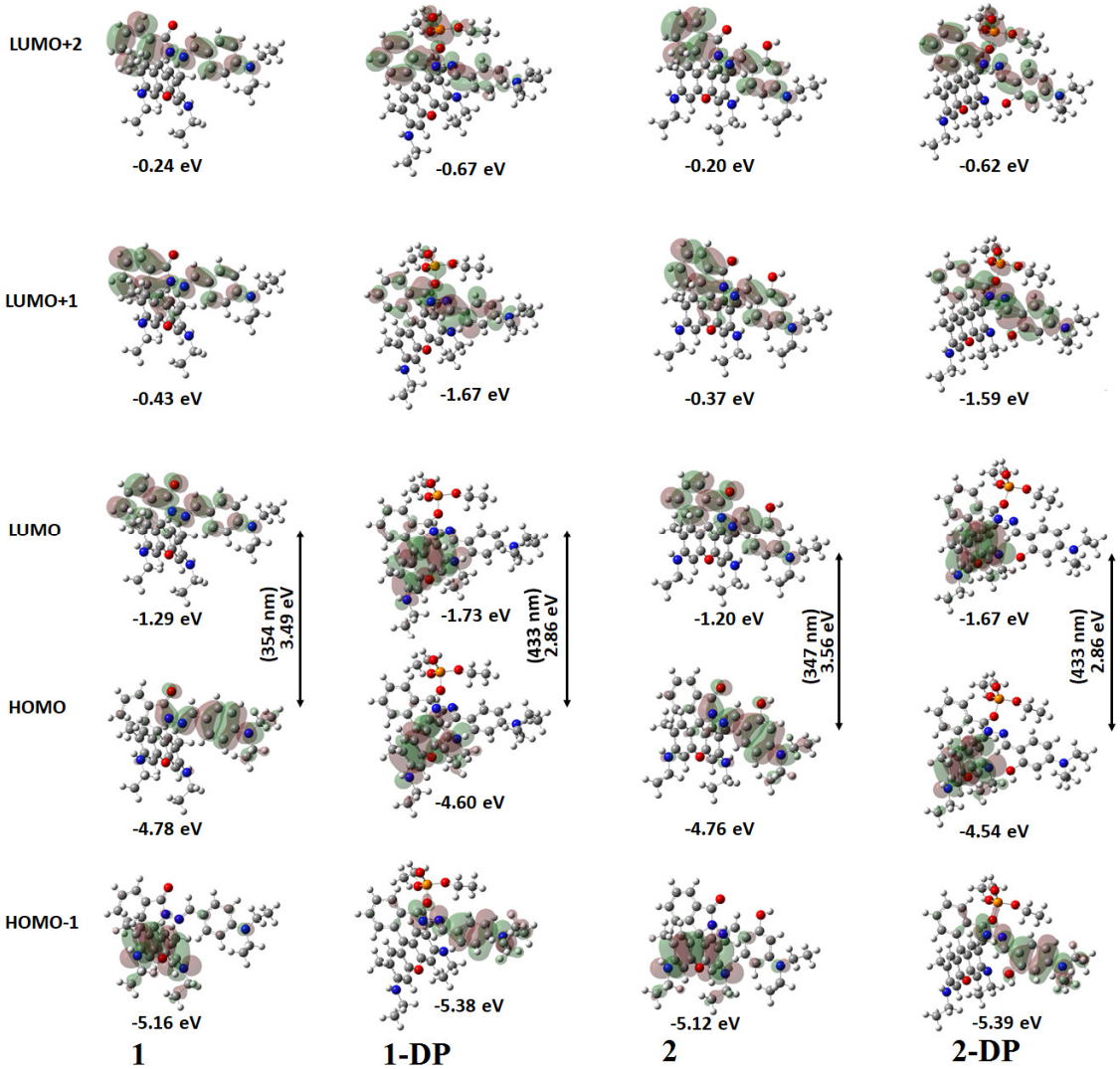

Fig. S36: Ground state MOs with corresponding distribution of π-electrons and energies of **1, 2** and their **1**-DP and **2**-DP adducts as elucidated from DFT calculations.

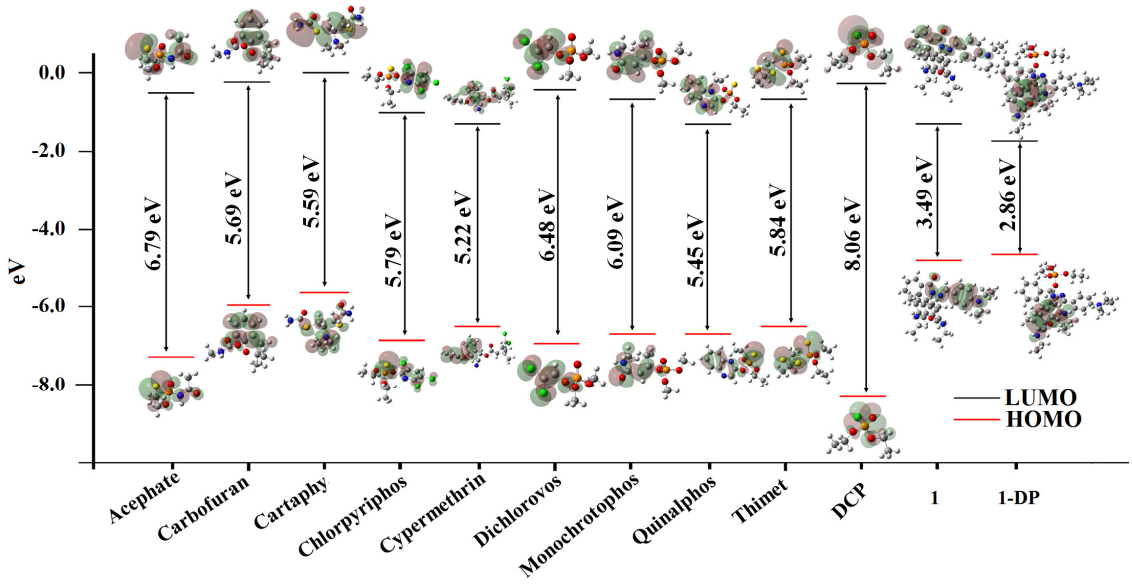

Fig. S37: Ground state HOMO-LUMO energy gap with corresponding distribution of π-electrons of various pesticides used in this study and their comparison to those of **1** and **1**-DP.

Table ST3: Ground state HOMO and LUMO energies and their transition energies (ΔE), corresponding chemical potentials($\Delta\mu_i$), dipole moments (μ_g), Mulliken charges over P-atoms estimated from the energy minimised structures of all the pesticides used in this study; those parameters of the probes (**1** and **2**) and their corresponding adducts (**1**-DP and **2**-DP). The units are mentioned in the parenthesis.

Probes/ analytes	Orbital Energy (eV)		Δ(ΔE), eV	$\Delta\mu_i$ (eV)	μ_g(D)	Mulliken Charge/e
	ΔE_{HOMO}	ΔE_{LUMO}	$\Delta E_{LUMO}-\Delta E_{HOMO}$	$(\varepsilon_{HOMO}+\varepsilon_{LUMO})/2$		
1	-4.788	-1.295	3.49	(-) 3.042	4.977	-0.579 (O_{sp})
2	-4.769	-1.205	3.56	(-) 2.984	5.495	-0.581 (O_{sp})
1-DP	-4.600	-1.734	2.86	(-) 3.167	8.798	--
2-DP	-4.541	-1.679	2.86	(-) 3.110	10.109	--
Acephate	-7.286	-0.494	6.79	(-) 3.890	4.135	1.087 (P)
Carbofuran	-5.924	-0.229	5.69	(-) 3.077	1.926	--
Cartaphy	-5.629	0.033	5.59	(-) 2.649	2.355	--
Chlorpyriphos	-6.854	-1.057	5.79	(-) 3.956	4.233	1.140 (P)
Cypermethrin	-6.491	-1.268	5.22	(-) 3.879	2.009	--
Dichlorovos	-6.918	-0.433	6.48	(-) 3.675	3.505	1.127 (P)
Monochrotophos	-6.713	-0.643	6.09	(-) 3.678	2.895	1.130 (P)
Quinalphos	-6.696	-1.245	5.45	(-) 3.921	4.500	1.132 (P)
Thimet	-6.486	-0.642	5.84	(-) 3.564	3.023	0.884 (P)
Diethyl-chlorophosphate (DCP)	-8.320	-0.257	8.06	(-) 4.288	4.650	1.181 (P)